Hydralab – Cornerdike

Influence of very oblique waves on wave overtopping

Patrick Oosterlo
4009711
Delft, March 2013
Delft University of Technology

Table of contents

Abstract

The objective of this report is to serve as a final report for my Bachelor thesis, with the main goals being determining the relation between very oblique wave attack and overtopping, and to accordingly adjust the formulae for oblique wave attack. The required knowledge to be able to read and understand this report is of a Bachelor in civil engineering level. All around the world different types of structures are built to protect adjacent areas from river or coastal flooding during high water levels. Only limited research is available on the influence of oblique wave attack (for angles over 45°) on wave overtopping. Hydralab is an EU-project, which gives researchers in the European Union the possibility to carry out research in large hydraulic facilities. Cornerdike is a part of the Hydralab IV program. The Cornerdike research project was performed at the shallow-water basin at DHI in Hørsholm, Denmark. To achieve the goal of this research, tests, data processing and analysis were done.

Acknowledgement

1. Introduction

In this chapter an introduction to this research report is given. The reasons for performing the research are described, the goal and research question are given and the build-up of the report is disclosed.

1.1. Introduction to Cornerdike

All around the world different types of structures are built to protect adjacent areas from river or coastal flooding during high water levels. The crest height of these structures is mostly determined by a design water level and wave run-up and/or wave overtopping. Only limited research is available on the influence of oblique wave attack (for angles of incidence over 45°) on wave run-up and wave overtopping due to the complexity and the high costs of model tests in wave basins. Only very few experiments are available and the available formulae show considerable differences for angels of wave attack over 45°. The definition of the angle of wave attack β can be found in figure 1.1. Most of the relevant research was performed on the influence of long crested waves and only few investigations are available on the influence of short-crested waves on wave run-up and wave overtopping (Pohl, 2011). Long crested waves have no directional distribution and wave crests are parallel and of infinite width. Only swell coming from the ocean can be regarded as a long crested wave. In nature, storm waves are short-crested. This means, that wave crests are not parallel, the direction of the individual waves is scattered around the main direction and the crests of the waves have a finite width.
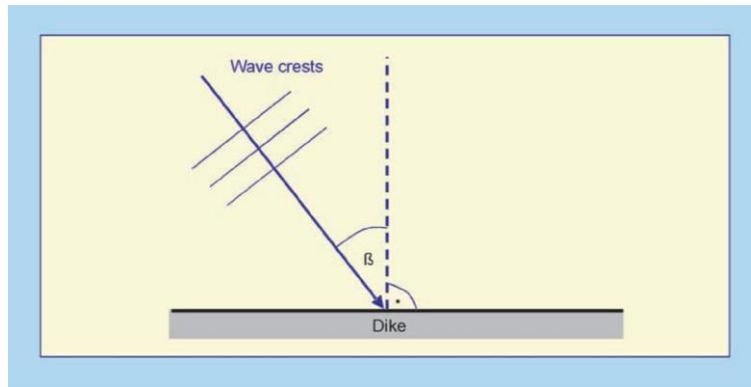
Fig. 1.1.: Definition of angle of wave attack β (Pullen et al., 2007).

Overtopping during angles of wave attack larger than 90° is possible. The main direction of the waves determines the angle of incidence, but because of the spreading in a wave field (short-crested waves), there always exist waves with other angles, which lead to other angles of attack. So even if the main direction is offshore (larger than 90°), there will always be waves that reach the structure. The amount of waves that still reaches the structure becomes smaller for larger angles of incidence. Currently, the most comprehensive source on wave overtopping is the European Overtopping Manual (EurOtop) (Pullen et al., 2007). In the European Overtopping Manual (EurOtop) (Pullen et al., 2007) it is described that, for oblique wave attack with angles over 45°, the wave overtopping will eventually be zero, if the angle of wave attack is large enough. For angles between 80° and 110° the wave height and wave period need to be lowered, due to diffraction. For angles larger than 110°, the crest height is allowed to be the same as the water level and the overtopping is set to zero (Pullen et al., 2007). For more information, see sections 2.1. and 2.2.

Examples of places in The Netherlands where oblique wave attack occurs, are the Dutch Wadden isles, the southern dike of the Noordoostpolder and the Ooster- and Westerschelde (Van der Meer, 2012c). Experimental data are required to estimate the wave run-up and wave overtopping behavior in these cases and to reduce the remaining uncertainties.

Cornerdike is a research that is part of the Hydralab IV program. Hydralab is an EU-project, which gives researchers in the European Union the possibility to carry out research in large hydraulic facilities. This has led to the fact that European universities have started partnerships and made research proposals. Cornerdike is a partnership between the universities of Dresden, Aken, Brno and Ghent and Van der Meer Consulting (Van der Meer, 2012c). The research on overtopping and run-up were both performed at the shallow-water basin at DHI in Hørsholm, Denmark. The tests for overtopping were performed in September 2012, the tests for run-up were performed in October 2012.

1.2. Goal of this report

The main research question of this report and of Cornerdike is:

What is the influence of short-crested very oblique waves on wave overtopping and how do the current design formulae need to be adjusted?

The hypothesis is as follows. The prediction is that the overtopping will be fairly similar to the values calculated with the design formulae, when the angles of incidence are still quite small. With the enlargement of the angles of incidence, the prediction is that the deviations will also become larger. The wave run-up and overtopping will become smaller with increasing angles of incidence, but will not become zero at 110°. The design formulae will need to be adjusted accordingly.

This leads to the goal of this report and of Cornerdike: The goal of this report and of Cornerdike is to determine the relation between very oblique wave attack and overtopping, and to accordingly adjust the design formulae for oblique wave attack.

1.3. Structure of this report

This report uses the overtopping research of Cornerdike and contains a first analysis of these research data. This report contains a short literature review, information on set-up and construction, instrumentation and calibration, test programs, information on data management, data processing and an analysis of the wave overtopping results.

The format of this report is as follows. In this report, first, a description of the project is given. Then, a literature review is presented in chapter 2. Next, the set-up and experimental procedures are described (chapter 3). The experimental procedures are described in chapter 4. In chapter 5, data processing is described. After that, in chapter 6, the analysis is described. Finally, conclusions are given in chapter 7. There are two appendices, A and B. Appendix A gives an overview of the test set-up and instruments. Appendix B gives an overview of all the tests and results.

The analysis consists of three parts. The first part of the analysis consists of comparing calculated overtopping discharge $q_{predicted}$ to measured overtopping discharge $q_{measured}$ for three different wave types, short-crested 1, short-crested 2 and long crested waves (see table 4.1.). In the second part the influence of the spreading width (see table 2.1.) is examined by comparing dimensionless overtopping discharges. Finally new empirical design formulae are determined.

2. Literature review

This chapter describes the current 'state-of-the-art' of design formulae and research on wave overtopping and oblique wave attack.

2.1. Information on overtopping

The most complete overview of tests and formulae for wave run-up and overtopping is the Overtopping Manual (EurOtop) (Pullen et al., 2007). The Overtopping Manual brings together information from other sources on overtopping during oblique wave attack, such as Technisch Rapport Golfoploop en Golfoverslag bij Dijken (TAW) (Van der Meer, 2002), Wave run-up and overtopping on coastal structures (De Waal & Van der Meer, 1992), Wave run-up and wave overtopping at dikes and revetments (Van der Meer & Janssen, 1994) and Wave run-up and overtopping (Van der Meer, 1998). The most important thing that can be derived from these sources is, that no good information is available for angles of wave attack larger than 90°. The information presented in this chapter is mostly from the Overtopping Manual (Pullen et al., 2007).

For wave overtopping considerations, the wave run-up R simply exceeds the crest height z. The wave overtopping is usually characterized by an overtopping discharge q per meter of the water defense, averaged over time. This discharge depends on:

- The wave height;
- The wave steepness;
- The slope;
- The existing freeboard.

The equation for the average overtopping discharge in probabilistic design and prediction or comparison of measurements is given by formula 2.1.:

$$\frac{q}{\sqrt{g \cdot H_{m0}^3}} = \frac{0.067}{\sqrt{\tan\alpha}} \cdot \gamma_b \cdot \xi_{m-1,0} \cdot exp\left(-4.75 \frac{R_c}{\xi_{m-1,0} \cdot H_{m0} \cdot \gamma_b \cdot \gamma_f \cdot \gamma_\beta \cdot \gamma_v}\right) \tag{2.1.}$$

with a maximum of:

$$\frac{q}{\sqrt{g \cdot H_{m0}^3}} = 0.2 \cdot exp\left(-2.6 \frac{R_c}{H_{m0} \cdot \gamma_f \cdot \gamma_\beta}\right) \tag{2.2.}$$

where:
q = average overtopping discharge [m³/s/m];
H_{m0} = estimate of the significant wave height from spectral analysis (=$4\sqrt{m_0}$) [m];
g = acceleration due to gravity (=9.81) [m/s²];
α = the angle of the structure slope with the horizontal [°];
R_c = crest freeboard of structure [m];
γ_f = correction factor concerning the roughness and permeability [-];
γ_b = correction factor concerning a berm with width B [-];
γ_β = correction factor concerning oblique wave attack [-];
γ_v = correction factor for a vertical wall on top of the crest [-];
$\frac{q}{\sqrt{g \cdot H_{m0}^3}}$ = dimensionless overtopping discharge [-];
$\frac{R_c}{H_{m0}}$ = relative crest freeboard [-].

The breaker parameter, also referred to as surf similarity or Iribarren number [-] is defined as follows:

$$\xi_{m-1,0} = \frac{\tan\alpha}{\sqrt{H_{m0}/L_{m-1,0}}} \tag{2.3.}$$

Where $L_{m,-1,0}$ is the deep-water wave length [m]:

$$L_{m,-1,0} = \frac{g \cdot T_{m-1,0}^2}{2\pi} \tag{2.4.}$$

where:
$T_{m-1,0}$ = average wave period [s].

The correction factor concerning oblique wave attack will be treated in greater detail in the next section. For an explanation of all the correction factors, see the Overtopping Manual (Pullen et al., 2007).

2.2. Information on oblique wave attack

For oblique waves the angle of wave attack is defined as the angle between the direction of propagation of waves and the axis perpendicular to the structure (for perpendicular wave attack $\beta=0°$), see figure 1.1. In the Overtopping Manual (Pullen et al., 2007) it is described that, for oblique wave attack with angles over 45°, the wave overtopping will eventually be zero, if the angle of wave attack is large enough. For overtopping calculations during oblique wave attack, the parameter γ_β represents the influence of the oblique wave attack. For overtopping and short-crested waves, the influence factor γ_β is calculated as follows:

$$\gamma_\beta = 1 - 0.0033|\beta| \; for: 0° \leq \beta \leq 80° \tag{2.5.}$$

No research is available for angles over 80°, so an estimation was made in TAW TR 2002 (Van der Meer, 2002):

$$\gamma_\beta = 0.736 \; for: |\beta| \geq 80° \tag{2.6.}$$

The influence factor γ_β for long crested waves holds:

$$\gamma_\beta = cos^2(\beta - 10°); (With \; estimations \; \gamma_\beta \geq 0.60 \; and \; \gamma_\beta = 1.0 \; for \; 0° \leq \beta \leq 10°) \; (\text{De Waal \& Van der Meer, 1992}) \tag{2.7.}$$

These estimations in formulae 2.5., 2.6. and 2.7. were not based on any information from research. However, it is true that, the larger the angle of incidence, the smaller the overtopping discharge becomes. For angles between 80° and 110° the wave height and wave period need to be adjusted, due to decreasing wave height (formula 2.8.) and wave period (formula 2.9.) when waves approach the structure:

$$H_{m0} \; is \; multiplied \; by \; \frac{110-|\beta|}{30} \tag{2.8.}$$

$$T_{m-1,0} \; is \; multiplied \; by \; \sqrt{\frac{110-|\beta|}{30}} \tag{2.9.}$$

Formula 2.8. creates a decreasing wave height, formula 2.9. creates a decreasing wave period, for angles of incidence $80° < |\beta| \leq 110°$. For angles larger than 110°, formulae 2.8. and 2.9. are set to zero, which leads to zero overtopping in formula 2.1. Thus, for angles larger than 110° the crest height is allowed to be the same as the water level (Pullen et al., 2007).

Figure 2.1. displays a summary of systematic research on the influence of oblique wave attack on wave run-up and wave overtopping under short-crested wave conditions.
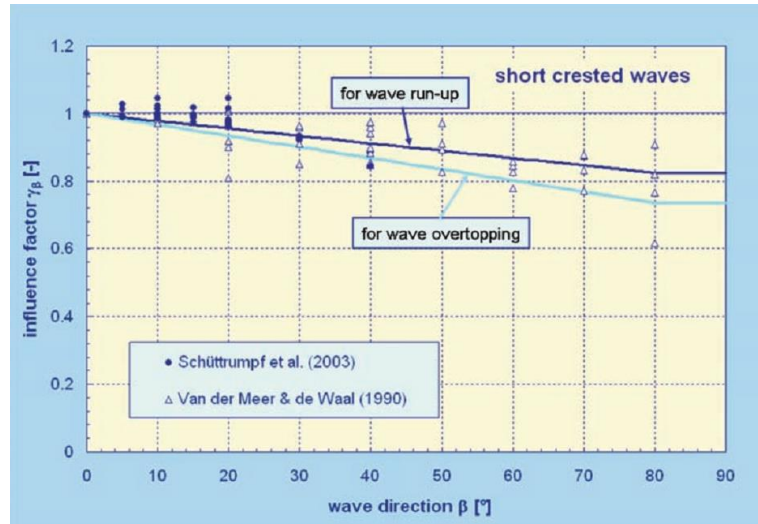
Fig. 2.1.: A summary of research on oblique wave attack under short-crested wave conditions (Pullen et al., 2007).

In figure 2.2. values of various influence (formulae 2.5. and 2.6.) and adjustment (formulae 2.8. and 2.9.) factors can be seen, for various angles of incidence. As one can see in the graph, the adjustment factors were chosen in a way that the wave height H_{m0} and wave period $T_{m-1,0}$ become zero at an angle of incidence of 110°, which leads to zero overtopping and run-up. All these procedures are, however, assumed procedures, and have never been validated.
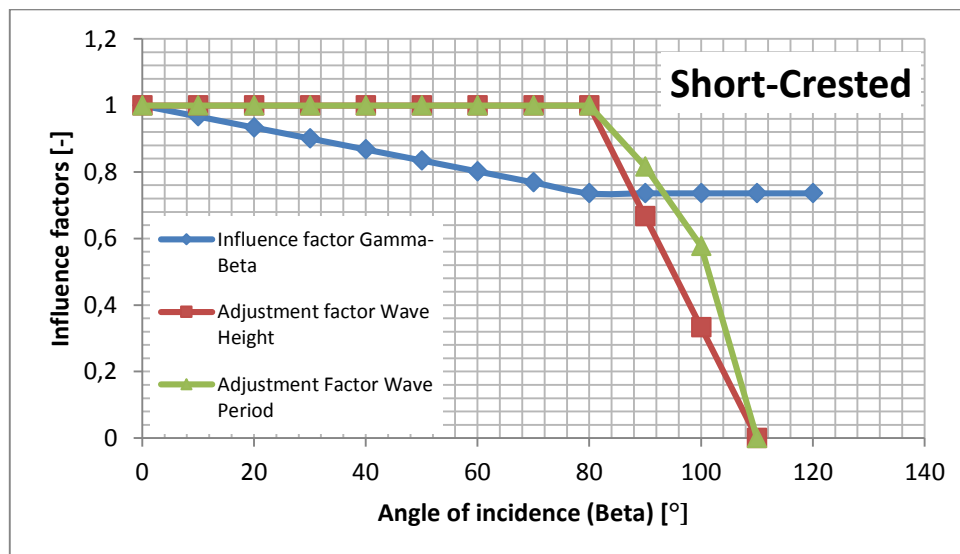
Fig. 2.2.: Influence and adjustment factors for oblique wave attack and short-crested waves, for various angles of incidence.

The directional spreading of wave fields might be characterized by the directional spreading width σ or the spreading factor *s*. Some properties of short-crested waves are that the wave crests are not parallel, the direction of the individual waves is scattered around the main direction and the crests of the waves have a finite length. Long crested waves have no directional distribution and wave crests are parallel and of infinite length. For long crested waves, the directional spreading width $\sigma=0°$ and the spreading factor $s=\infty$, see table 2.1.

A distribution function is necessary to be able to generate short-crested waves. This distribution function indicates the spreading around the main direction. A model that was used in previous research is the *cos-2s-model* (Van der Meer, 2012b):

$$D(f,\theta) = A(f)\, cos^{2s}\big((\theta - \theta_m)/2\big)$$

(2.10.)

Where:
$D(f,\theta)$ = the distribution function of directional spreading [-];
$A(f)$ = a function dependent of *s*, which leads to a constant for a certain chosen spreading [-];

2s = spreading factor, coefficient larger than 1 [-];
θ = the direction of wave propagation [°];
θ_m = the main direction of wave propagation [°].

The value of *2s* determines whether the distribution is narrow or wide. A small value of *2s* leads to a wide distribution, a large value of *2s* leads to a narrow distribution.

For the analysis of directional distribution data, often a normal distribution with corresponding standard deviation σ is used. According to Sand and Mynett (Sand & Mynett, 1987) the relation between *2s* and σ is:

Spreading factor *2s* [-]	Spreading width σ (°)
2	65
4	51
10	34
20	25
80	12
∞	0 (long crested)

Table 2.1.: Relation between 2s and σ according to Sand and Mynett (De Waal & Van der Meer, 1990).

Thus, often the short-crested wave field is generated with the *cos-2s-model* and the analysis is done on basis of the spreading σ (De Waal & Van der Meer, 1990).

3. Set-up and instrumentation

An overview of the set-up and instrumentation for the tests of Cornerdike can be found in this chapter. Also, the calibration procedures are described.

3.1. Set-up of Cornerdike
In this section, the set-up for Cornerdike is covered.

- Basin

For Cornerdike the shallow water wave basin at DHI in Hørsholm, Denmark was used. The length of the basin is 35 m, the width is 25 m and the maximum water depth is 0.9 m. Gravel was placed along the edges of the basin to provide absorption of the waves. Figures 3.1. and 3.2. show an overview of the basin.

Fig. 3.1.: Overview of the shallow wave basin at DHI.

Fig. 3.2.: Overview of the basin, dike and set-up for Cornerdike.

- Wave generator

The wave generator that was used for Cornerdike was 22 m long, and consisted of two parts, one of 18 m and one of 4 m. The wave generator could be controlled and programmed by a computer running the wave generation software of DHI, called AWACS. Figure 3.3. shows the wave generator.

Fig. 3.3.: Wave generator at DHI.

- Dike

The concrete dike had a slope of 1:4 and was divided into two parts, connected by a corner (see figure 3.7.). In figure 3.4. can be seen that one part is almost normal in relation to the wave maker (N-dike), the other part is almost parallel to the wave maker (P-dike). The whole dike is rotated 15° relative to the wave maker. The water levels and crest heights were chosen according to the characteristics of the basin. They had to be chosen in such a way that there would always be overtopping, but not too much. The expected overtopping discharges were larger at the P-dike than at the N-dike, because the angles of incidence were smaller at the P-dike than at the N-dike. Thus, the crest height of the P-dike was set to 75 cm and the height of the N-dike was set to 70 cm. A short overview of the set-up on the dike is given in figures 3.5. and 3.6. For a complete overview of the locations of the dike and all devices see Appendix A.

Fig. 3.4.: Overview of set-up and definition of the N- and P-dike (Pohl & Krüger, 2012a).

Fig. 3.5.: Experimental set-up with locations of different devices (Pohl & Krüger, 2012b).
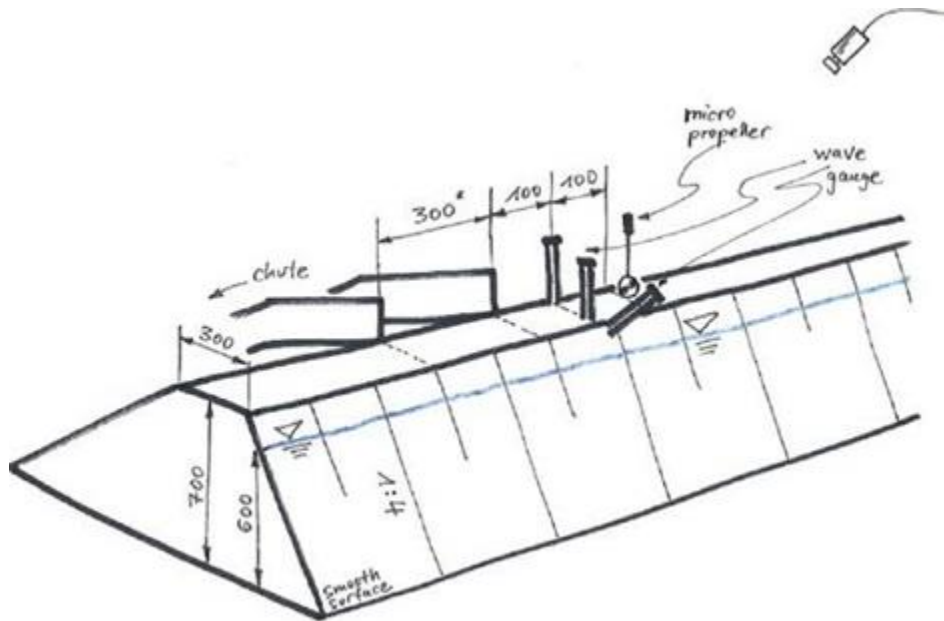
Fig. 3.6.: Experimental set-up on the crest (Pohl & Krüger, 2012a).

Fig. 3.7.: The dike in a dry basin (Pohl & Krüger, 2012a).

- Overtopping boxes

During Cornerdike five overtopping boxes were used. The boxes were mounted on a load cell to be able to determine the overtopping volume and the individual overtopping wave volumes. The overtopped water was transported by means of chutes. The chutes at the P-dike were 10 cm wide and the chutes at the N-dike were 30 cm wide, so that there would always be overtopping, but not too much. The overtopping boxes consisted of two parts: an inner and an outer box. The outer box contained the inner box, the load cell and an automatic pump. The function of the outer box is to keep the inner box dry. The inner box contained a controllable pump and a mat, which reduces the measurement peaks of the falling water. The dimensions of the inner boxes were 0.75 m x 0.75 m x 0.43 m (Pohl & Krüger, 2012a). The overtopping boxes and chutes are the same ones that were used for the FlowDike research (Lorke et al., 2010). For an overview of an overtopping box, with inner and outer box, chute and pumps, see figure 3.8.

Fig. 3.8.: Overtopping box with pumps and chute.

3.2. Instrumentation of Cornerdike

The instruments used for Cornerdike are described in this section. The sampling frequency for all the instruments (and thus the data) was 40 Hz. For a complete overview of all the devices and their locations see Appendix A.

- Load cells

Five load cells were used to measure the amount of overtopped water. The load cells were mounted under the inner overtopping boxes. A load cell has a height of approximately 10 cm and gives a signal in Volt. The load cells were calibrated in such a way that an increase of 20 kg gave an increase of 1 V. The maximum capacity of a load cell was 2150 N. The accuracy of a load cell is approximately 0.05%.

- Pumps

Eleven pumps were used to empty the inner and outer overtopping boxes. All outer boxes contained one automatic pump. First, the inner boxes also contained one controllable pump, but an extra pump was placed in overtopping box 3 during the tests, because the overtopping was too large. The inner boxes contained controllable pumps, which were turned on when the overtopped water reached a certain level, and were turned off before the pump started sucking air. The capacities of the pumps were determined before the testing started. The pump in box 1 had a capacity of 1.72 l/s, the capacity of pump 2 was 3.30 l/s, the combined capacity of the pumps in box 3 was 3.39 l/s, the capacity of pump 4 was 1.75 l/s, and of pump 5 was 1.60 l/s. During the data processing, the amount of pumped out water was added to the amount of water in the overtopping box, see chapter 5.

- Wave gauges

A total of 40 wave gauges were used. A wave gauge is a device which can determine wave height, water level elevation and flow depth. The wave gauge measures a change of conductivity between two thin, parallel stainless steel electrodes. The conductivity changes proportionally to changes in the surface elevation of the water between the electrodes (Lorke et al., 2010). A wave gauge gives a signal in Volt. The wave gauges were calibrated in such a way that an increase of 10 cm gave an increase of 1 V. The wave gauges were placed in wave arrays. A wave array is a row of wave gauges. The wave arrays contained three or five wave gauges. To be able to analyze a short-crested wave field, the gauges were placed in a pentagon arrangement in a 5-wave gauge array, and the gauges were placed in a triangular arrangement in a 3-wave gauge array. The wave gauges at the crest were placed one behind the other. Figure 3.9. shows three wave gauges and a propeller.

- Propellers

Six propellers were used. Propellers are based on the concept of an impeller. The rotations of the fan were measured and transformed to an output signal in Volt (Lorke et al., 2010). The propellers had a range of 0.04 – 5 m/s and an accuracy of 2%. There was a propeller at every overtopping chute.

- Acoustic Doppler Velocity meters (ADV's/Vectrino)

Four ADV's were used. An ADV is a current meter, which measures the current using the Doppler effect. The transmitter generates a short pulse of sound at a known frequency. The energy of the pulse passes through the sampling volume. Part of this energy is reflected by suspended matter along the axis of the receiver, where it is sampled by the velocity meter, whose electronics detect the shift in frequency (Lorke et al., 2010). The range that was used for the ADV's was ±100 cm/s, the sampling frequency was 40 Hz and the resolution 1 mm/s.

Fig. 3.9.: Three wave gauges and a propeller on the crest.

3.3. Calibration procedures

Calibration was done every morning and between tests according to the following schedule:

Every morning:
- Checking the water level: The water level needed to be checked to make sure it was correct according to the next test (60, 65 or 68 cm);
- Calibration of the load cells: Every morning a weight of 20 kg was placed in each of the overtopping boxes and the resulting signal value (an increase of 1 V) was checked;
- Calibration of the wave gauges: Every morning all wave gauges were calibrated. The gauges were placed one wave array at a time on a stand which was then put in a bucket of water. The values of the signals were recorded. After that the gauges were lowered into the bucket. The signals were recorded again. Then, the gauges were raised again, and the signals were recorded once more. The recorded signals were compared to each other. When the difference between the signals was very close to zero, the calibration file was saved and applied and the wave gauges were returned to their normal location;
- Checking the range of the ADV's: Every morning the configuration of the ADV's was checked for the right range and sampling frequency (±100 cm/s and 40 Hz);
- Offset of the wave gauges, propellers, load cells: The values of the wave gauges, propellers and load cells were set to zero. The first offset file of every day was saved.

Before every test:
- Checking the water level: The water level needed to be checked to make sure it was correct according to the next test (60, 65 or 68 cm);
- Emptying the overtopping boxes: After every test, the overtopping boxes were emptied;
- Blowing out the propellers: Before every test someone blew into the propellers a few times, to undo them from remaining water and to check if the propeller blades could turn freely;
- Offset of the wave gauges, propellers, load cells: The values of the wave gauges, propellers and load cells were set to zero. The offset was applied.

4. Experimental procedures and test program

In this chapter, the build-up of the test program and experimental procedures of Cornerdike are described.

The overtopping and run-up have been measured for tests, which, each time, consist of different sets of wave parameters. The test program of Cornerdike consisted of 30 test series. In total 129 tests were done. The water levels d were 60, 65 and 68 cm. The crest height of the N-dike was 70 cm and the height of the P-dike was 75 cm. This resulted in crest freeboards of 10 and 15 cm for water depth d=60 cm, of 5 and 10 cm for d=65 cm and of 2 and 7 cm for d=68 cm. The significant wave heights H_{m0} were 7, 10 and 15 cm and the angles of the waves relative to the wave maker $\beta_{wavemaker}$ were 0, 7.5, ±15, 22.5, ±30, 37.5 degrees. The resulting angles of incidence at the dike β_{dike} were 0°, 7.5°, 15°, 22.5°, 30°, 45°, 60°, 75°, 82.5°, 90°, 97.5°, 105° and 112.5°. There were six different types of wave conditions. The waves consisted of three main types of crest widths, short 1, short 2 and long crested waves, and one of the two different steepness's s_{0p}. Each of the 30 test series for Cornerdike consisted of a bundle of the six different waves, which are described in table 4.1. For an overview of all the tests and their results, see Appendix B.

wave number w_x [-]	wave type [-]	spreading factor s [-]	spreading width σ [°]	steepness s_{0p} [-]
w1	short 1	5	34	0,025
w2	short 1	5	34	0,05
w3	short 2	40	12	0,025
w4	short 2	40	12	0,05
w5	Long	∞	0	0,025
w6	Long	∞	0	0,05

Table 4.1.: The different waves used for Cornerdike.

The wave maker was controlled by a computer running a wave synthesizer program, DHI AWACS, in which the test parameters could be entered. The angle of the waves relative to the wave maker, the spreading factor, the steepness, the wave height and the water depth were entered in the wave synthesizer program. Furthermore, the duration of the test was entered and the programming file was saved. The waves were generated with the *cos-2s-model* (Van der Meer, 2012b) and the analysis will be done with σ according to Sand and Mynett (Sand & Mynett, 1987), see section 2.2.

5. Data processing and storage

The acquired data are processed and analyzed to determine the effect of very oblique wave attack on run-up and wave overtopping. These procedures are described in this chapter.

The instruments were placed in wave arrays, which contained three or five wave gauges. All the instruments were connected to amplifiers and Analog/Digital-converters (A/D-converters), the amplifiers and converters were connected to a computer by a serial cable. The computer ran the DHI Wave Synthesizer program, with which all the signals could be monitored in real-time, the offset and calibration could be done, and with which all the data was stored. The wave generator could be controlled and programmed by another computer.

The sampling frequency for all the instruments was 40 Hz, the measured units of measurement are:
- Mass: e.g. weight of the overtopped water (load cells);
- Length: e.g. water level elevations (wave gauges);
- Time: e.g. test/pumping durations (computer);
- Speed: e.g. water velocities (propellers and ADV's);
- Frequency: e.g. sampling frequency (computer);
- Voltage: e.g. signals of instruments (A/D-converters).

The data recording and wave generation were started at the same time by means of a countdown, so that the data recording started with a steady state of the basin water. The data recording ran one minute longer than the wave generation, so that the data recording also ended with a steady water state. For the data processing, a 'constant process' was necessary. A constant process means that the data processing needs to start and end with full wave generation. Thus, during the data processing, the start and end times were redefined.

The data were stored in files with the *dfs0* extension. The data files contain all the data and can be opened in MIKE Zero. MIKE is a software package developed by DHI. The file names that have been used are of the format [test series][number]_w[wave number]_[minus/plus][wave angle]_[wave height]_[water depth]. So for example, ts05_w1_m150_015_60 means test series 5, wave short 1 (long period), angle -15°, significant wave height 15 cm, water depth 60 cm.

In Mike, the zero levels and crossing levels for all propellers and wave gauges were determined. Zero levels are the levels at which the device should give a zero value, crossing levels are levels above which the data are reliable, and below which the data are unreliable, for example because of noise. The zero and crossing levels were noted in Excel files. With the help of Mike, the measured wave heights, wave periods and angles of incidence could be determined for every wave array. The zero and crossing levels were later also used to perform a Crossing analysis, Directional wave analysis and Wave reflection analysis for every test in Mike, which will be used in the final Cornerdike report, but are not included in this report.

After that, the *dfs0*-files were exported to *ASCII*-files (table files) in Mike. The *ASCII*-files were then renamed to *daf*-files. The *daf*-files contain the same information as the *dfs0*-files, but in a table format. The *daf*-files could be accessed by a Matlab *m*-file, which was a customized version of a Hydralab Flowdike file. The *m*-file was used to calculate the overtopping and adjust the amount of overtopped water for when pumps were running. The amount of overtopped water was adjusted with the capacity of the pumps multiplied by pump run times (see section 3.2. for the capacities of the pumps). Thus, the file calculated the pumped volume per overtopping box, volume of water in each of the boxes and the overtopping discharge per box.

Finally, all the results were collected in an Excel-file called summarize_data_org.xls. This file contains all the data, for example test names, test numbers, wave heights, wave numbers, water levels, wave directions, wave parameters, overtopping information, wave array parameters, and analysis information.

6. Analysis

In the analysis of this report, predicted overtopping is compared to measured overtopping, the influence of the spreading width is examined and first empirical adjustments to the design formulae are given.

6.1. General analysis information

The results of the tests should be compared to existing research and literature. From chapter 2 it can be concluded that, in short, the larger the angle of incidence β becomes, the smaller the overtopping discharge becomes. The existing design method says that for angles of incidence β larger than 80°, the wave height H_{m0} and the wave period $T_{m-1,0}$ need to be adjusted, see formulae 2.8. and 2.9. The result of these adjustments is, that according to the current formulae, the wave height and wave period become zero at β=110°, and thus the overtopping discharge also becomes zero at 110° (Pullen et al., 2007).

As mentioned in section 1.2., the goal of this report and of Cornerdike is to determine the relation between very oblique wave attack and overtopping, and to accordingly adjust the formulae for the oblique wave attack influence and adjustment factors.

The correctness of the entered wave parameters (and thus waves) was measured in front of the wave maker. When the angle of incidence comes close to, or becomes larger than 90°, the wave field at the dike will not be equal to the entered wave field, because the wave height and wave period decrease when approaching the dike. This is also why the adjustment factors are included in the current design theory.

In a memo (Van der Meer, 2012a) to the Cornerdike partners, J.W. Van der Meer provided a set-up for a first analysis of the results. In this memo it is stated that, due to the fixed test set-up not all instruments will give correct values at all times, because they might be out of the correct wave field or might be influenced by reflection at the corner. This leads to wrong wave heights, wave periods, angles of incidence and thus to wrong overtopping discharges. According to the memo, for this first analysis, wave gauges 16-20 are used as the wave conditions for the total wave field. Due to the location of wave gauges 16-20, they are less influenced by reflection and are always in the correct zone of the wave field. The H_{m0} and $T_{m-1,0}$ from these gauges can be used for a first analysis. The same holds for the overtopping boxes. The boxes are sometimes also out of the correct wave field and will not always give correct overtopping discharges. In the memo, an overview is given, see also figure 6.1. For this first analysis only overtopping boxes 4 and 5 are used, because these are the boxes that are the farthest from the corner, and will be least influenced by diffraction at the corner. The overtopping discharges from boxes 4 and 5 can be used for a first analysis.

Fig. 6.1.: Overview of reliability of test results at overtopping boxes (Van der Meer, 2012a).

Excel files were made for the analysis. One table is an overview of all the tests and results. This table contains the information of all the tests, the results from all the tests (of which the information for wave gauges 16-20 and overtopping boxes 4 and 5 was used), and the calculated overtopping for all the tests. The measured wave height and wave period from wave gauges 16-20 were used for the calculations. The table can be found in Appendix B.

The accuracy of the load cell (0.05%, see section 3.2.) combined with the maximum measuring range (approximately 220 kg, see section 3.2.) leads to a detectable load of 0.11 kg. Using the maximum test duration

of 2040 s and the chute width of 0.30 m leads to a detectable overtopping of 0.11/(2040·0.30) = 0.00018 l/(s·m). A value lower than this 'detectable load' value will be neglected.

Due to the different accuracies of the instruments, and due to the fact that in previous research (Lorke et al., 2010) was observed, that sometimes a difference of a factor 2 in the overtopping of two boxes next to each other occurs, without any apparent or explainable reasons, it is very difficult to determine 'a measurement accuracy'. The difference between overtopping boxes overrules all other accuracies, and therefore no error bars will be included in the graphs.

In the analysis, first, the predicted overtopping discharge $q_{predicted}$ is compared to measured overtopping discharge $q_{measured}$ for the three different wave types, short-crested 1 (spreading width $\sigma=34°$), short-crested 2 (spreading width $\sigma=12°$) and long crested (spreading width $\sigma=0°$). The properties of these waves can be found in table 4.1. After that, the influence of the spreading width is examined by comparing the dimensionless mean overtopping discharges $q/(gH_s^3)^{0.5}$ for the different spreading widths. Finally, first empirical adjustments to the design formulae are given.

6.2. Measured overtopping versus calculated overtopping
From the tables with all the tests and results six more tables were made, which only contained the test results from short 1, short 2, or long crested waves. From these tables six graphs were made, figure 6.2. to figure 6.7. The figures show calculated wave overtopping versus measured overtopping, for the different waves (spreading 34°, 12° and 0°) and overtopping boxes 4 and 5. The axes are both on a logarithmic scale. Distinction has been made between the various angles of wave attack. Values on the line means that predictions match measured values. Values below the line give smaller measured values than predicted. For values above the line the measured overtopping is larger than the predicted overtopping.

Overtopping box 4
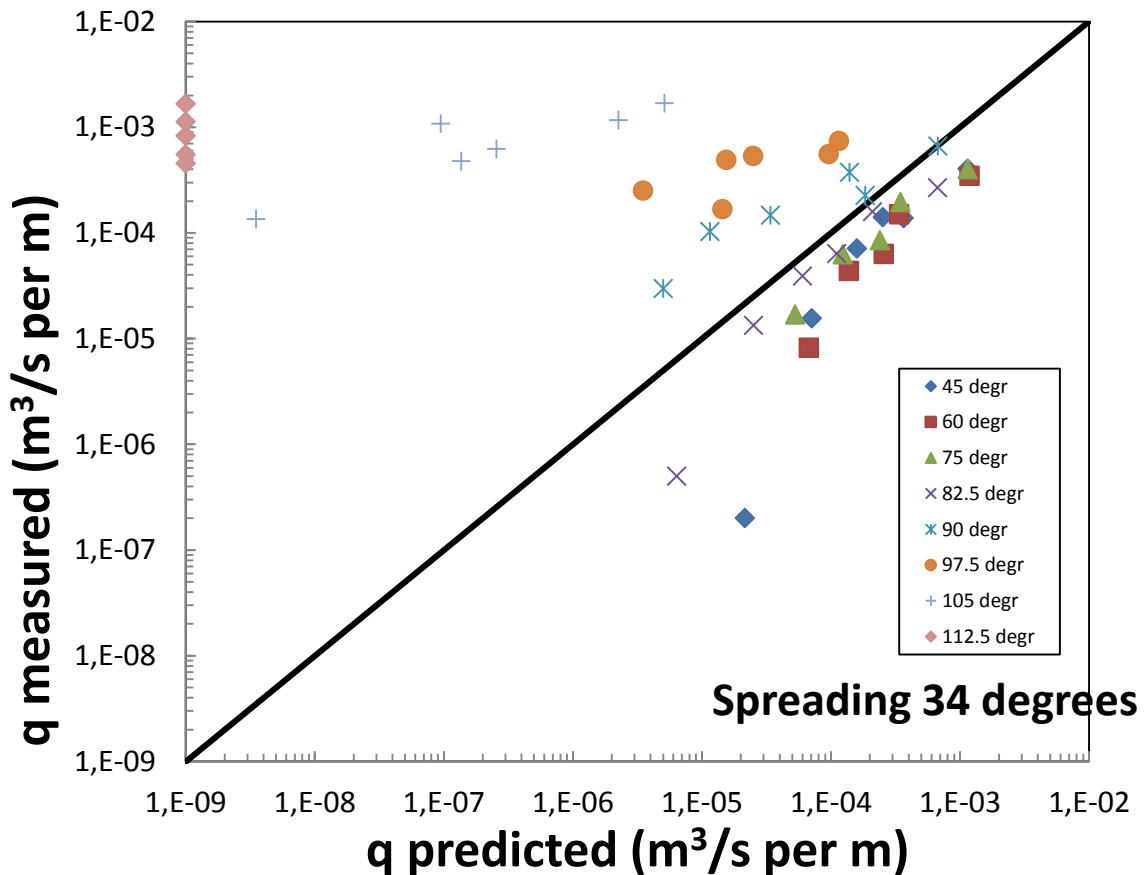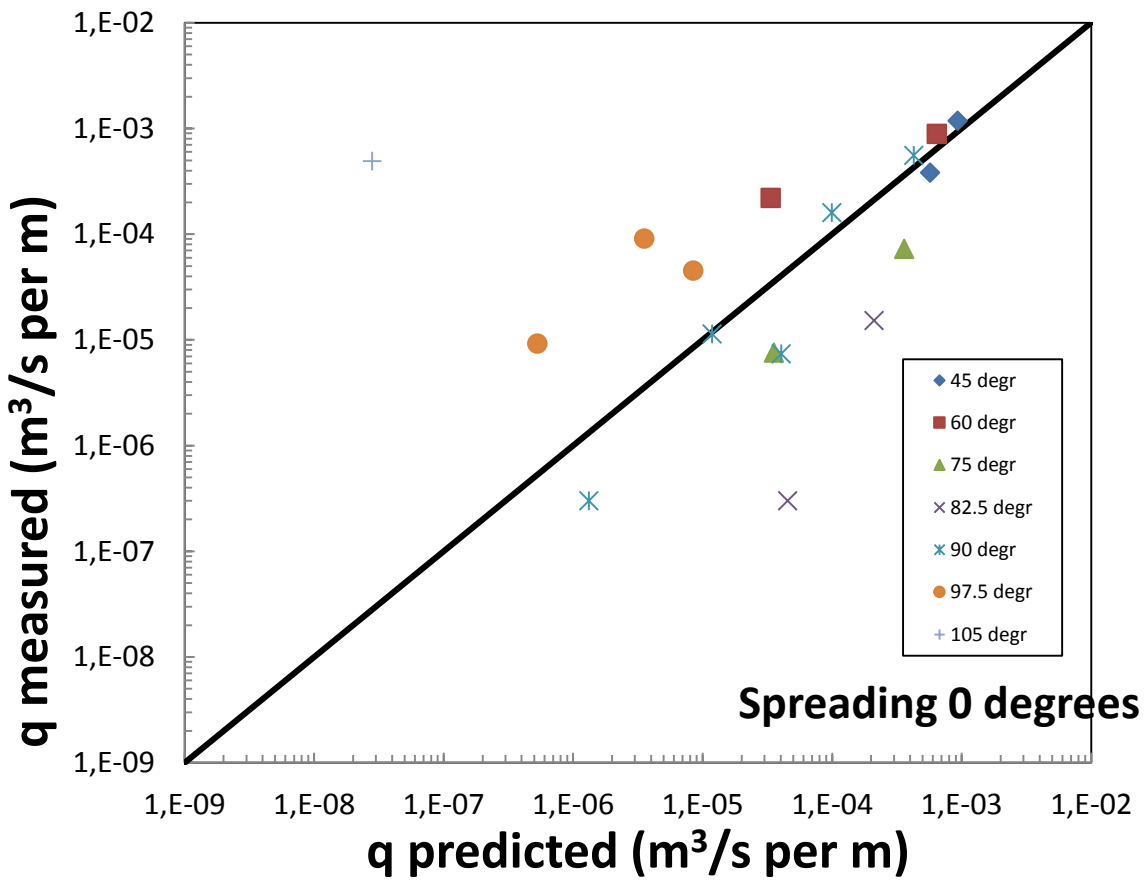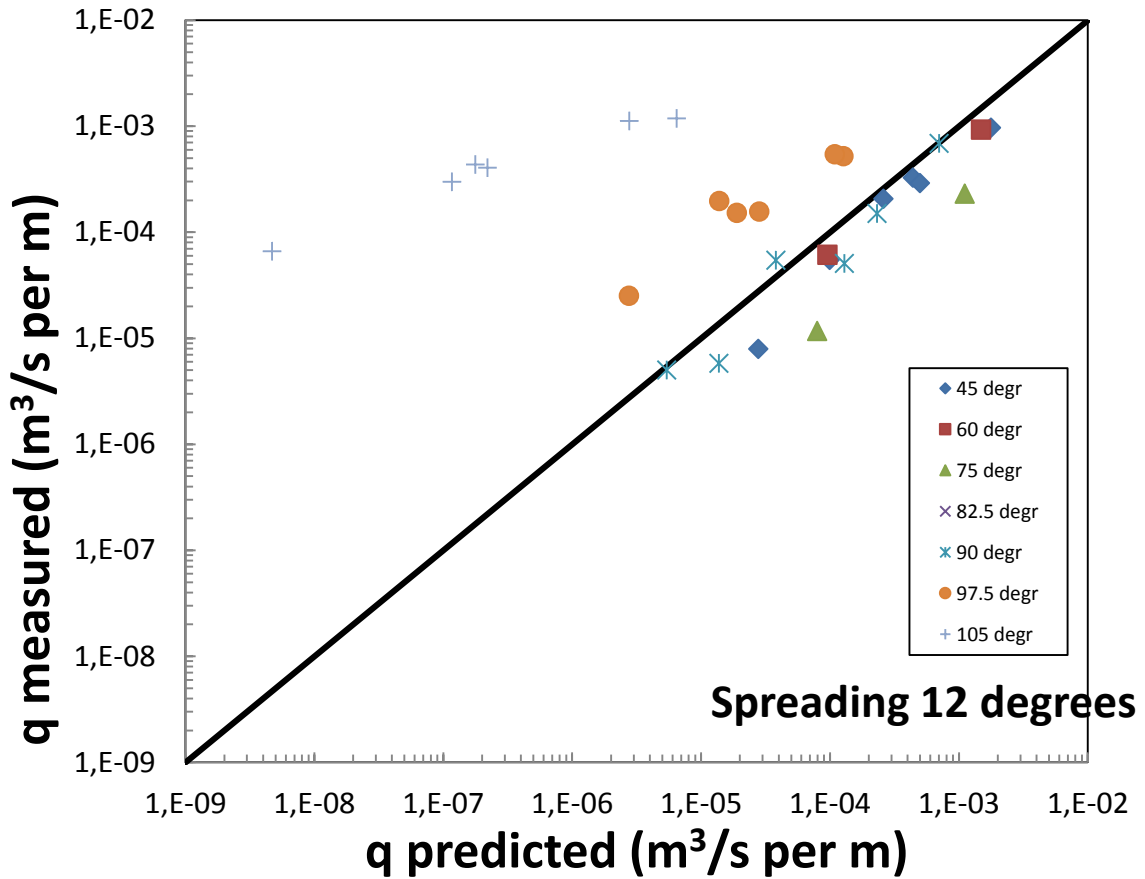
Fig. 6.2., 6.3., 6.4: Graphs showing calculated overtopping vs. measured overtopping, for overtopping box 4 for spreading 34, 12, 0 degrees.

From these graphs, the following observations can be made:

1. The values match quite well, with a few exceptions. The values for the short-crested waves match much better than the values for the long crested waves. This is probably due to diffraction at the corner and the difficulty of absorbing and not causing resonance with long crested waves;

2. The values of the measured overtopping for angles of wave attack between 45° and 82.5° for a spreading of 34° are lower than the predicted overtopping, roughly a factor of 3. A notable fact is, that the values of the measured overtopping for angles of incidence from 45° - 82.5° are all of about the same size. The values for 90° are above the line. Measured overtopping for angles of wave attack between 45° and 90° for a spreading of 12° matches predicted overtopping well. For these angles of incidence the values are all around the line. For a spreading of 0°, the measured overtopping for angles of incidence between 45° and 90° differs significantly from predicted overtopping. In this range of angles of wave attack it was expected that measurements and predictions should match quite well, because good data in this area are available. The data for the spreading of 34° and 12° do indeed match quite well, but the spreading of 0° does not. This could be due to the reason given in the previous point;

3. For all three spreading widths, for angles of wave attack larger than 90°, the values are all above the line, indicating that overtopping does not decrease as fast as theory predicts. It looks like the values for angles of 90° and above are all on one horizontal line. For 112.5° the data points were positioned on the vertical axis for a measured value of 10^{-9}, because the prediction in reality is zero (which cannot be plotted on a logarithmic scale). Measured values were clearly not zero and are in the same order of magnitude as for 90° - 105°. However, a fact that could have had influence is that, for large angles of wave attack, the crest freeboard was decreased to only 2 cm (see section 4.1.). Further analysis is necessary to be able to determine the influence of this fact.

Overtopping box 5
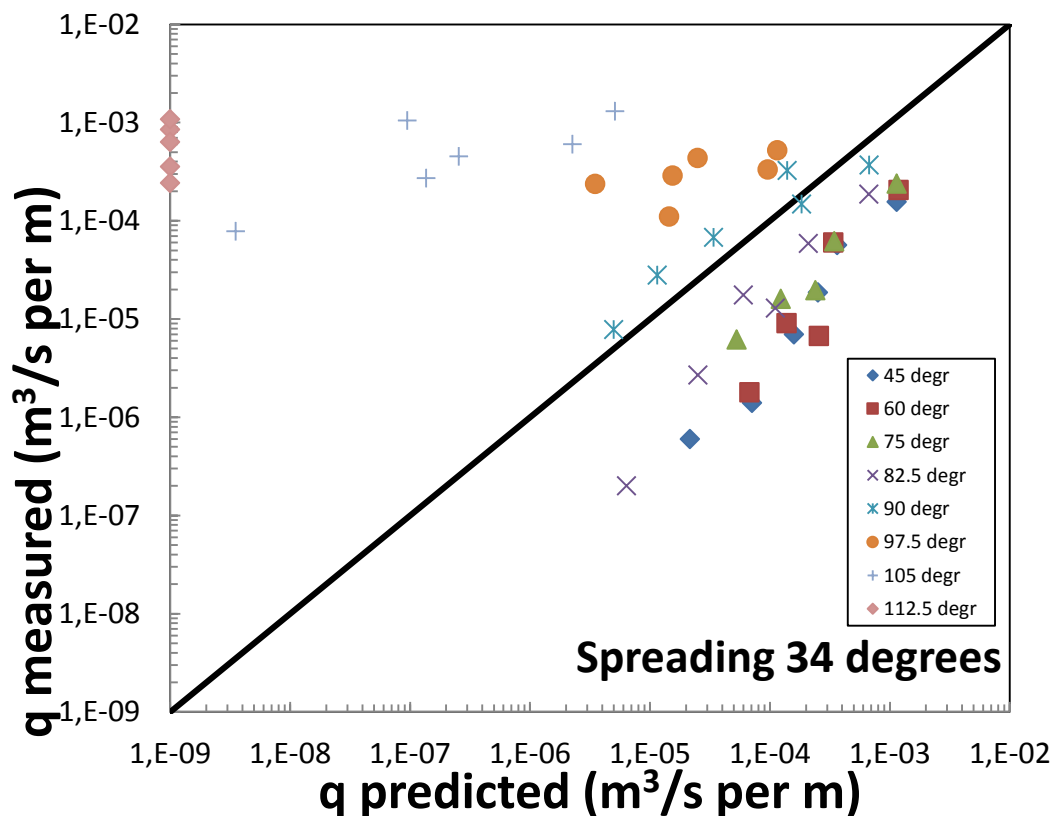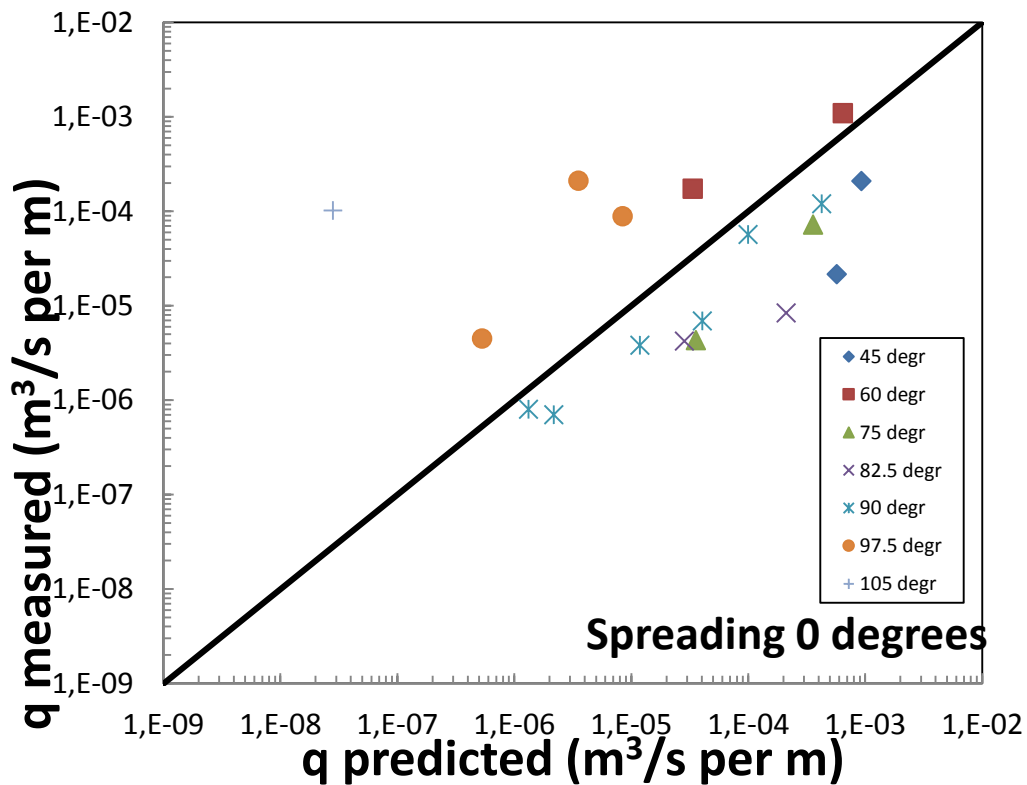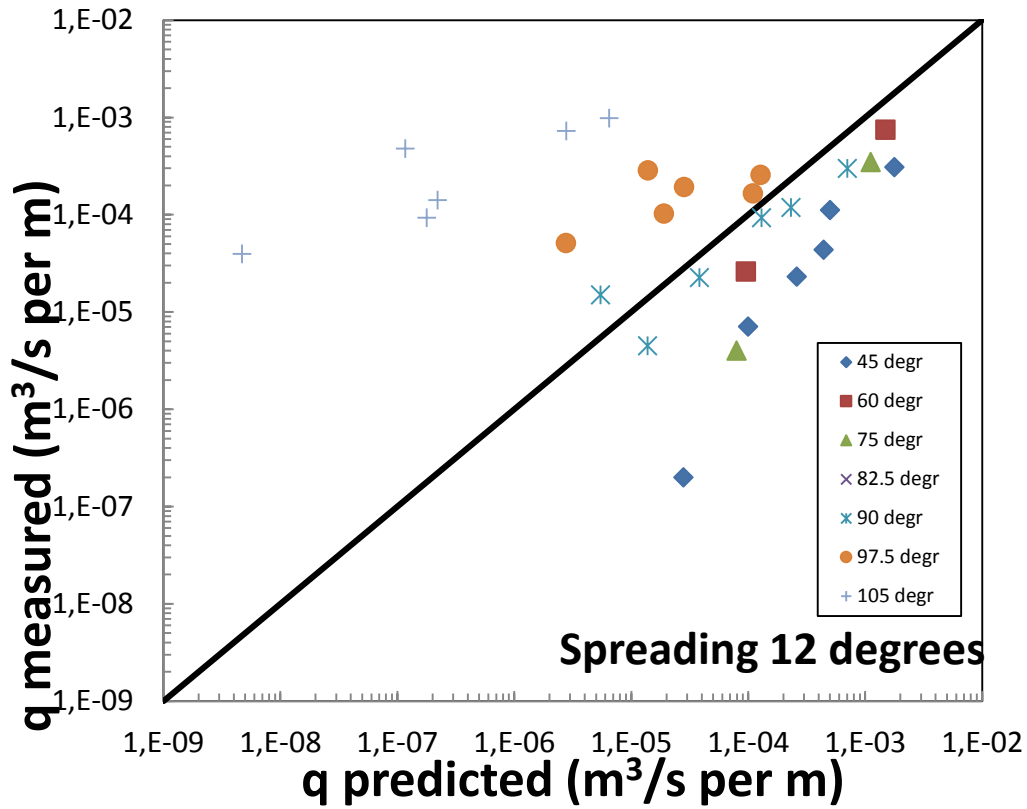
Fig. 6.5., 6.6., 6.7: Graphs showing calculated overtopping vs. measured overtopping, for overtopping box 5 for spreading 34, 12, 0 degrees.

From these graphs, the following observations can be made:

4. The measured overtopping values are too low. The values for the short-crested waves match better than the values for the long crested waves. The difference between short-crested and long crested is probably due to diffraction at the corner and the difficulty of absorbing and not causing resonance with long

crested waves. Why the values at box 5 are too low needs to be further analyzed. However, as mentioned before in section 6.1., an explanation could be, that in previous research (Lorke et al., 2010) was observed that sometimes a difference of a factor 2 in the overtopping of two boxes next to each other occurs, without any apparent or explainable reasons;

5. The measured values for 45° are not reliable and are too low, for all three spreading widths (under the line in figures 6.5., 6.6. and 6.7.), because the wave field could not be generated properly at box 5 (see figure 6.1.). At this angle of incidence, Box 5 was not completely under direct wave attack, because the corner of the dike caused diffraction;

6. For a spreading of 34° and 12°, measured overtopping for angles of wave attack between 45° and 82.5° is significantly lower than predicted (under the line in the figures). A notable fact is, that the values of the measured overtopping for angles of incidence from 45° - 82.5° are all about the same size. The values for 45° are just a little smaller than for 60°. For a spreading of 0°, the values of measured overtopping for angles of incidence from 45° - 90° are also lower than predicted, except for 60°, these are higher than the predicted values. In this range of angles of wave attack it was expected that measurements and predictions should match quite well, because good data in this area are available. The difference between measured and predicted is roughly a factor of 10. This could be due to the observation in previous research (Lorke et al., 2010) mentioned in point 4, but has to be analyzed in more detail;

7. At 90° measured and predicted values match quite well for a spreading of 34° and 12° (all around the line in the figures), but this may be just by accident as for smaller angles of wave attack there is an unexpected deviation (see previous point);

8. For all three spreading widths, for angles of wave attack larger than 90°, the values are, just like with box 4, all above the line, indicating that overtopping does not decrease as fast as theory predicts. Again, it looks like the values for angles of 90° and above are all on one horizontal line. Again, a fact that could have had influence is that, for large angles of wave attack, the crest freeboard was decreased to only 2 cm (see section 4.1.). Further analysis is necessary to be able to determine the influence of this.

6.3. Influence of the spreading width

From the tables with all the tests and results another six tables and graphs were made, comparing the different spreading widths. Dimensionless mean overtopping discharges $q/(gH_s^3)^{0.5}$ are compared for the three different spreading widths 34°, 12° and 0°, and again for boxes 4 and 5. By using the dimensionless overtopping discharges, the influence of the wave height is discounted. Again, both axes are on a logarithmic scale. Distinction has been made between the various angles of wave attack. Values above the line means that the dimensionless overtopping discharge is larger for the larger spreading width. Values below the line means that dimensionless overtopping is larger for the smaller spreading width.

According to the current theory and previous research (De Waal & Van der Meer, 1990), long crested waves with angles of incidence 0° - 30° cause virtually the same wave overtopping as with perpendicular attack. Outside of this range, the reduction factor decreases fairly quickly to $\gamma_\beta = 0.6$ at $\beta = 60°$. With short-crested waves the angle of wave attack has less influence. This is mainly caused by the fact that within the wave field the individual waves deviate from the main direction β. The influence factor for short-crested waves decreases linearly to $\gamma_\beta = 0.736$ at $\beta = 80°$. The overtopping should decrease faster for long crested waves as for short-crested waves, with increasing angle of incidence. As mentioned in section 2.1., no information is known for angles over 90°. Thus, according to the theory, for the lower angles of incidence, the overtopping should be approximately the same for all three spreading widths, but for the higher angles of incidence, the overtopping should be higher with larger spreading widths: overtopping 34° > 12° > 0°.

Overtopping box 4
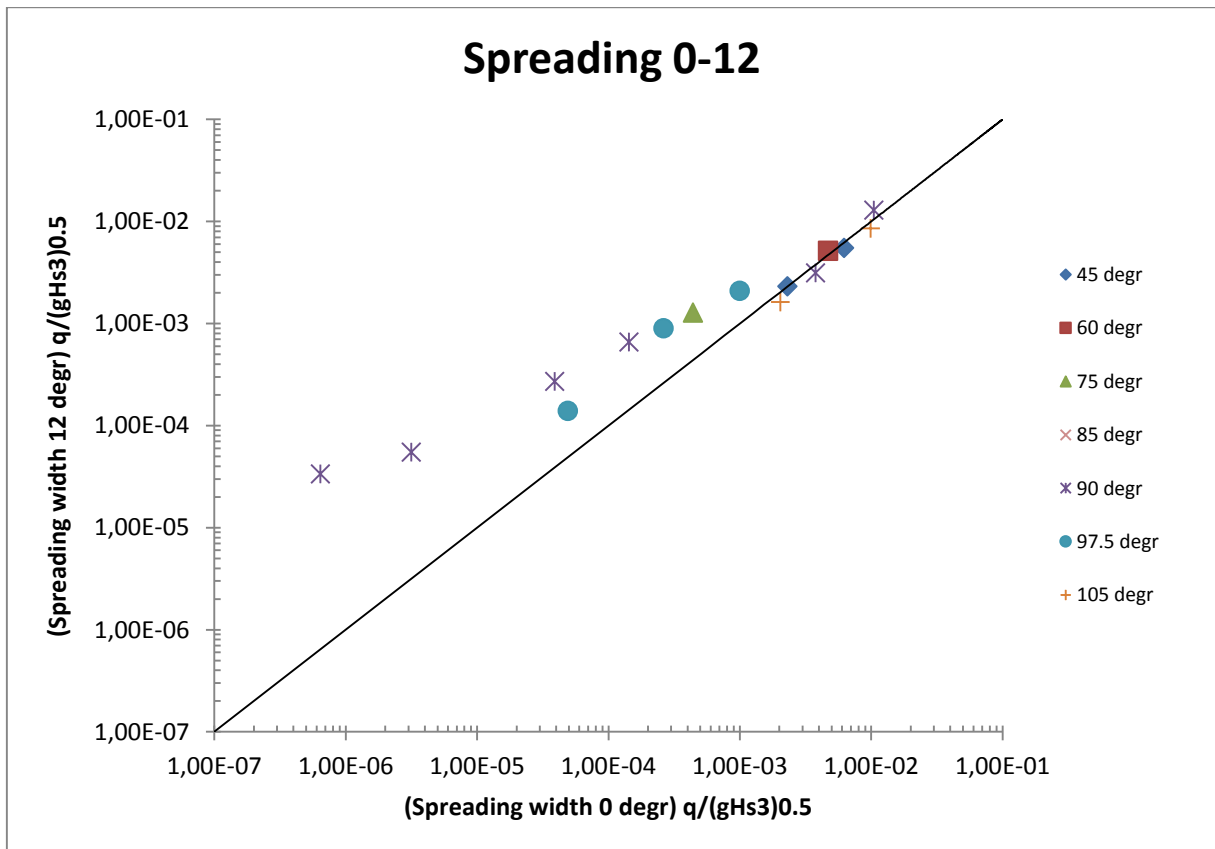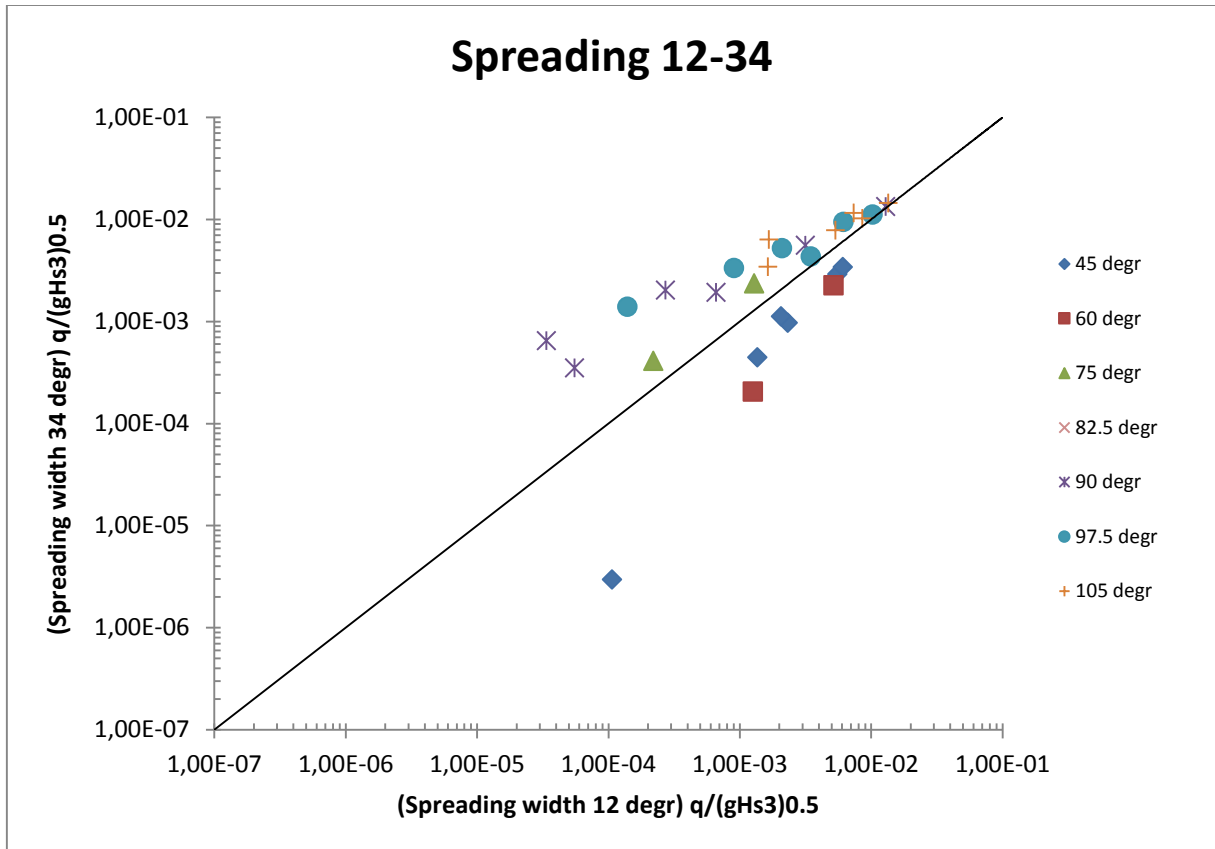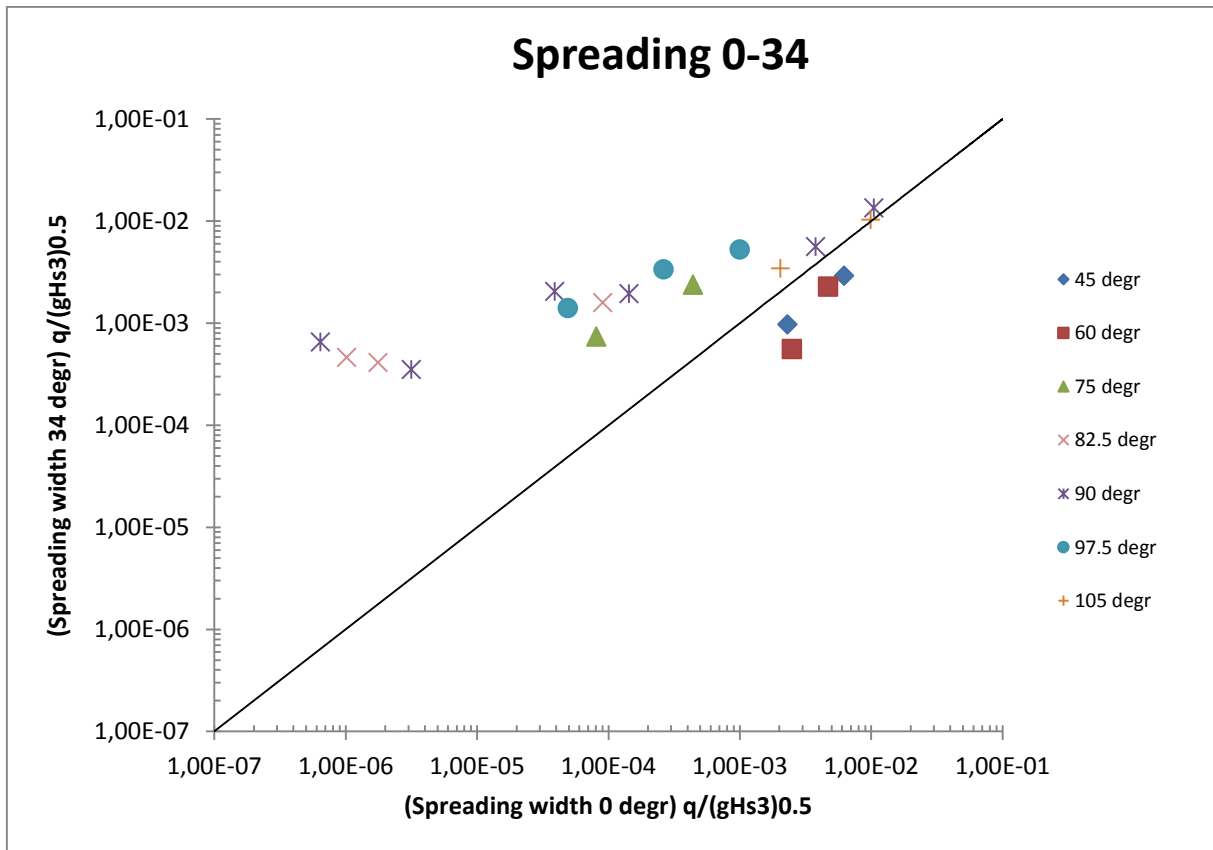
Fig. 6.8., 6.9., 6.10.: Graphs comparing dimensionless overtopping for the different spreading widths, for overtopping box 4.

From these graphs, the following observations can be made:

1. The values for 45° and 60° are on the line in the graph for a spreading of 0° and 12°, which means they are of the same magnitude, which is according to the theory. However, for these angles of incidence, the values for a spreading of 34° are smaller;

2. The values for the larger angles of incidence are above the lines in the graphs, which is according to the theory, overtopping values for spreading 34° > 12° > 0°;

3. The values for 105° (for which no previous research is available) are close to the lines in the graphs, which means that the values are of approximately the same magnitude for all three spreading widths. This could mean that for very large angles of incidence, the influence of the spreading decreases again, however this has to be analyzed in more detail. Also, these values are fairly high, which means that overtopping does not decrease as fast as the current theory predicts, and does certainly not become zero. Again, a fact that could have had influence is that, for large angles of wave attack, the crest freeboard was decreased to only 2 cm (see section 4.1.). Further analysis is necessary to be able to determine the influence of this.

Overtopping box 5

Spreading 12-34
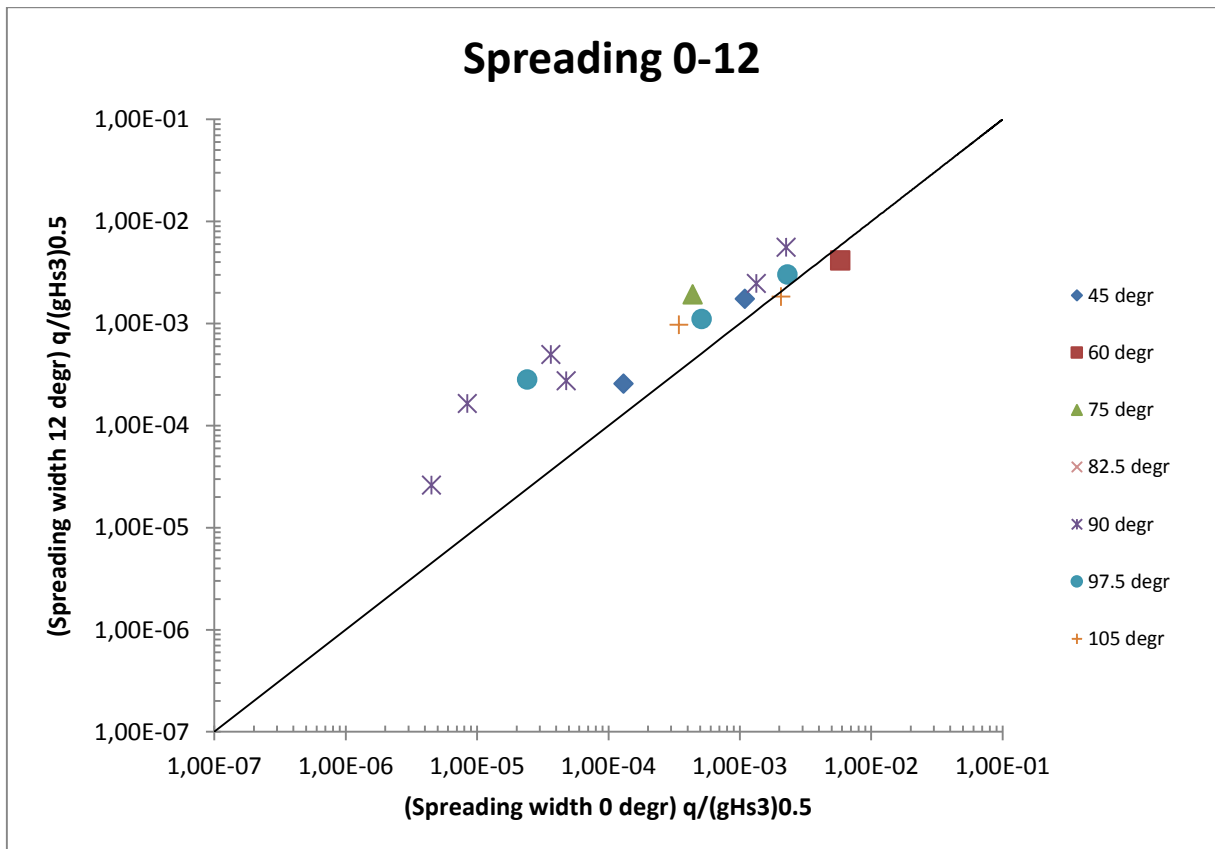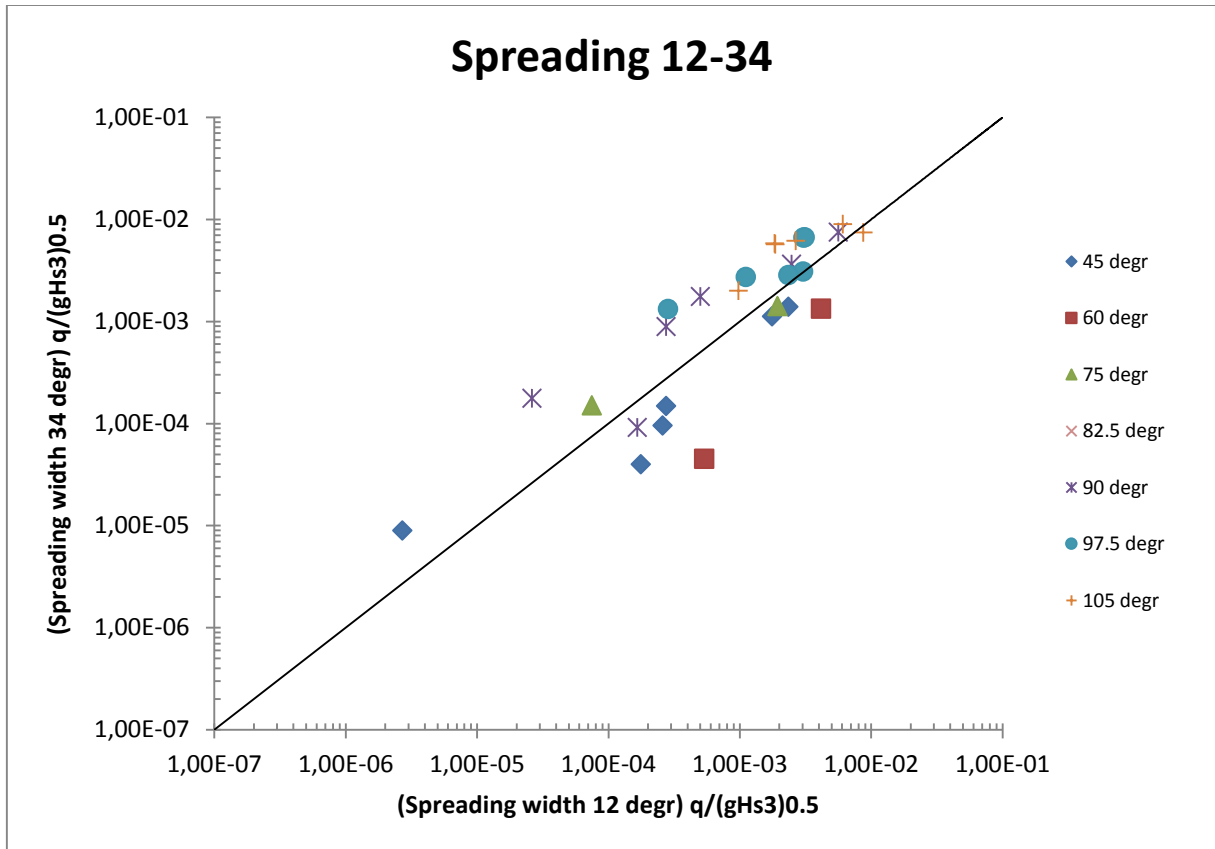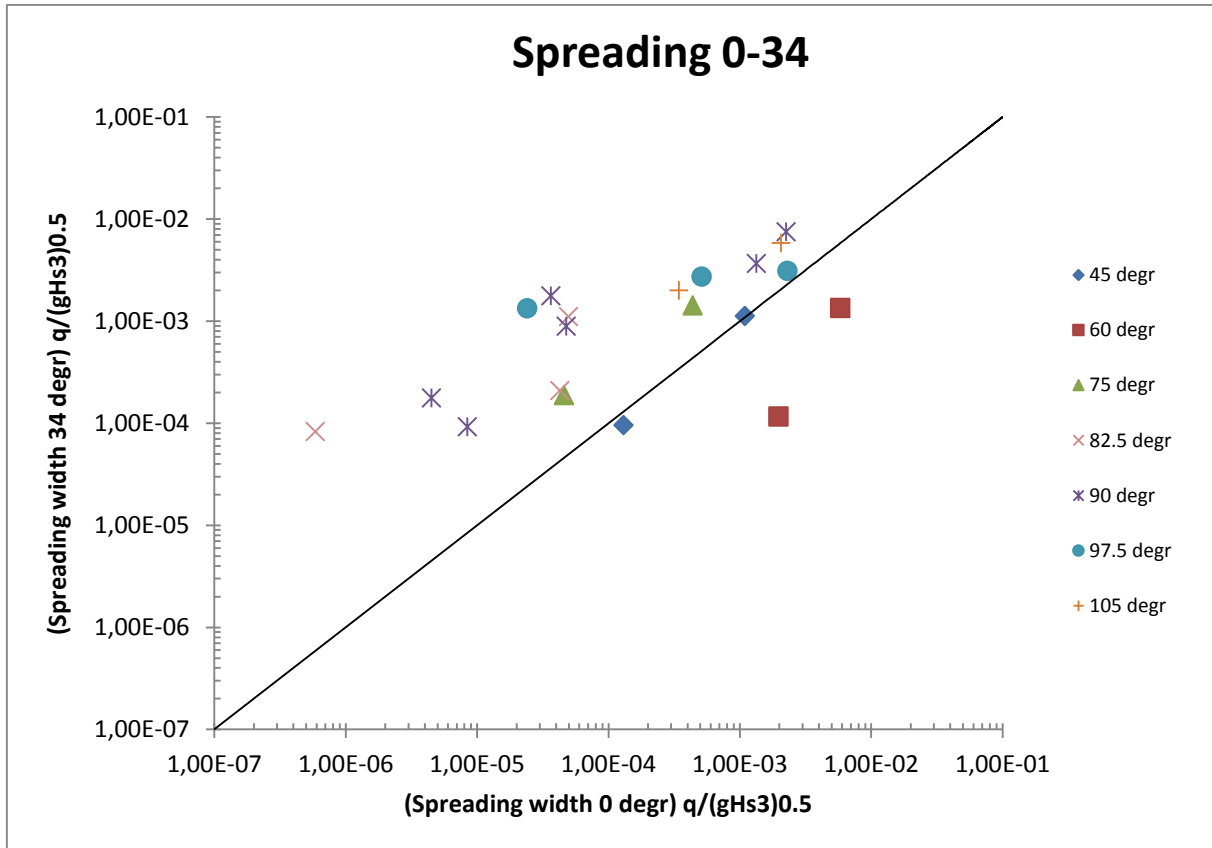
Spreading 0-12

Fig. 6.11., 6.12., 6.13.: Graphs comparing dimensionless overtopping for the different spreading widths, for overtopping box 5.

From these graphs, the following observations can be made:

4. Again, the values for 45° and 60° are of the same magnitude for a spreading of 0° and 12°, which is according to the theory. For a spreading of 34°, the values for 45° are also of the same magnitude, but the values of 60° are smaller;

5. The values for 75° are of approximately the same magnitude for a spreading of 12° and 34°, these values are larger than the values for a spreading of 0°, which is according to the theory;

6. The values for the larger angles of incidence are above the lines in the graphs, which is according to the theory, overtopping values for spreading 34° > 12° > 0°;

7. The values for very large angles of incidence (97.5° and 105°) are again fairly close to the lines in the graphs, which again seems to point to the fact that the influence of the spreading decreases for very large angles of incidence. Just like with box 4, these values are fairly high, which again means that overtopping does not decrease as fast as the current theory predicts, and does certainly not become zero.

6.4. First empirical estimates

In this section new empirical design formulae will be determined, for short-crested waves, using the previous two sections, 6.2. and 6.3. Only the data from overtopping box 4 and spreading width 34° will be used, because the values from box 5 are too low, and thus unreliable (points 2, 4, 5, 6 and 7 in section 6.2.). Why this difference between boxes 4 and 5 is present, needs to be analyzed in more detail. It looks like the values for angles of 90° and above are all on one horizontal line. The measured overtopping for these angles of incidence was larger than the predicted overtopping, and did certainly not become zero at 110° (points 3 and 8 of section 6.2. and points 3 and 7 of section 6.3.).

The old adjustment factors can be found in section 2.2., formulae 2.8. and 2.9.

The first thing that needs to be adjusted is the value of 110°. The overtopping does not become zero at this angle, so as a first estimate, 180° is taken.

The next thing to do, is getting the predicted values in accordance with the measured values (on the line in the graphs). This is done by iteration (trial and error). This leads to the new adjustment factors of:

$$H_{m0} \text{ is multiplied by } \frac{180-|\beta|}{110} \tag{6.1.}$$

$$T_{m-1,0} \text{ is multiplied by } \sqrt{\frac{180-|\beta|}{110}} \tag{6.2.}$$

When these new adjustment factors are used with the old formulae for the influence factor γ_β (formulae 2.5. and 2.6., see section 2.2.), this leads to the following graph:
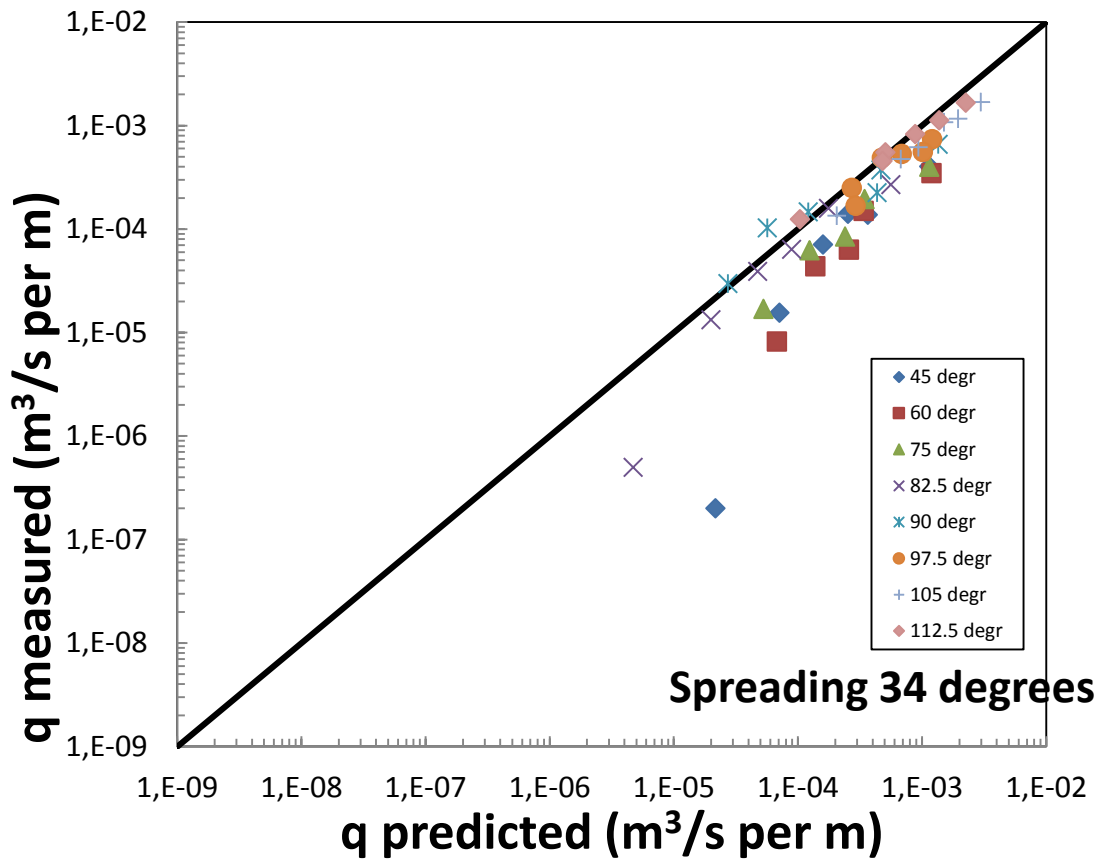
Fig. 6.14.: Graph comparing predicted and measured overtopping, using new adjustment factors, for spreading 34 degrees, for box 4.

Now, the data for the larger angles of incidence are on the line, but the values for the lower angles of incidence are still under the line (points 2, 4, 5 and 6 of section 6.2.). Thus, another adjustment is necessary. To get the values for the lower angles of incidence on the line in the graph, the following influence factor γ_β (found by iteration) is used in combination with the new adjustment factors (formulae 6.1. and 6.2.):

$$\gamma_\beta = 1 - 0.0060|\beta| \; ; \; \left(\gamma_\beta \geq 0.60\right) \tag{6.3.}$$

This leads to the following graph:
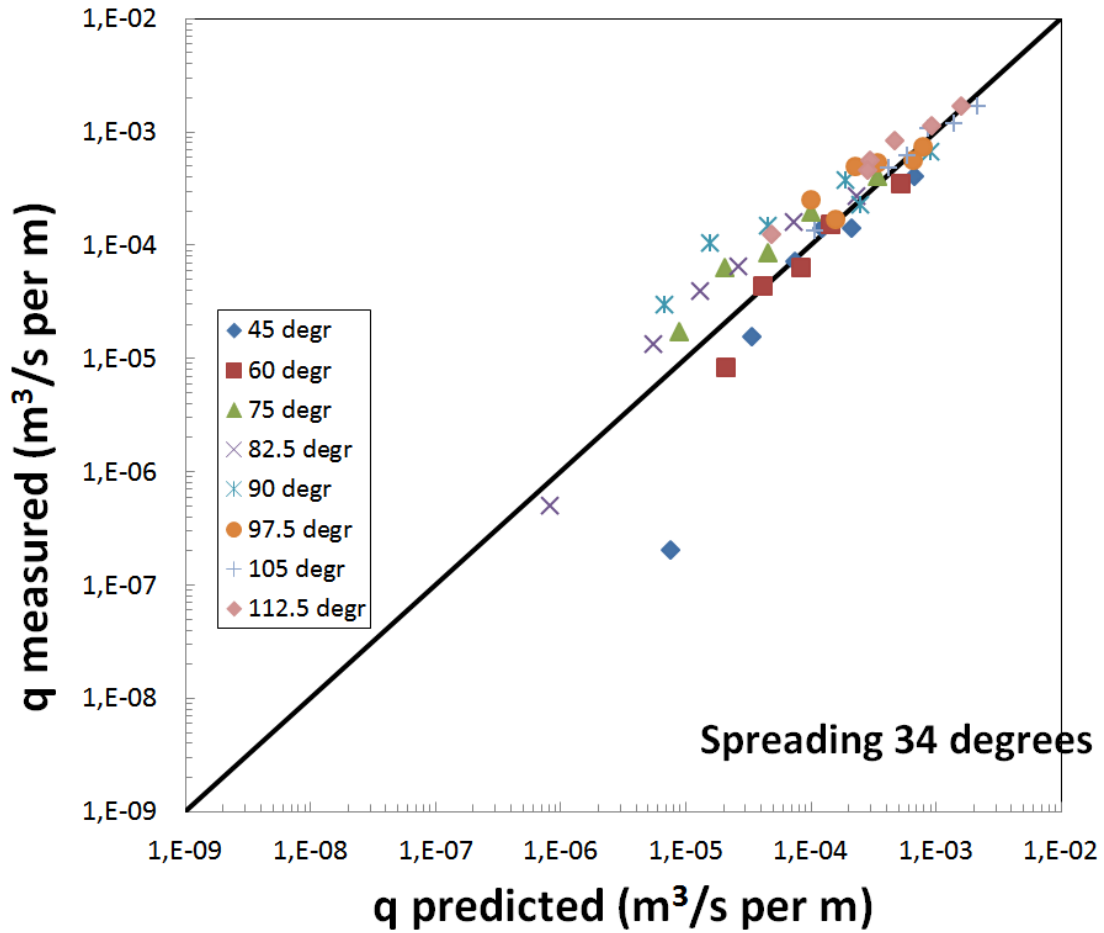
Fig. 6.15.: Graph for predicted vs. measured overtopping, using new adjustment and influence factors, for spreading 34 degrees, for box 4.

However, now the values for the larger angles of incidence are not on the line anymore. Therefore, another small adjustment to the adjustment factors is suggested (found by iteration):

$$H_{m0} \text{ is multiplied by } \frac{180-|\beta|}{100} \tag{6.4.}$$

$$T_{m-1,0} \text{ is multiplied by } \sqrt{\frac{180-|\beta|}{100}} \tag{6.5.}$$

This leads to the following graph:
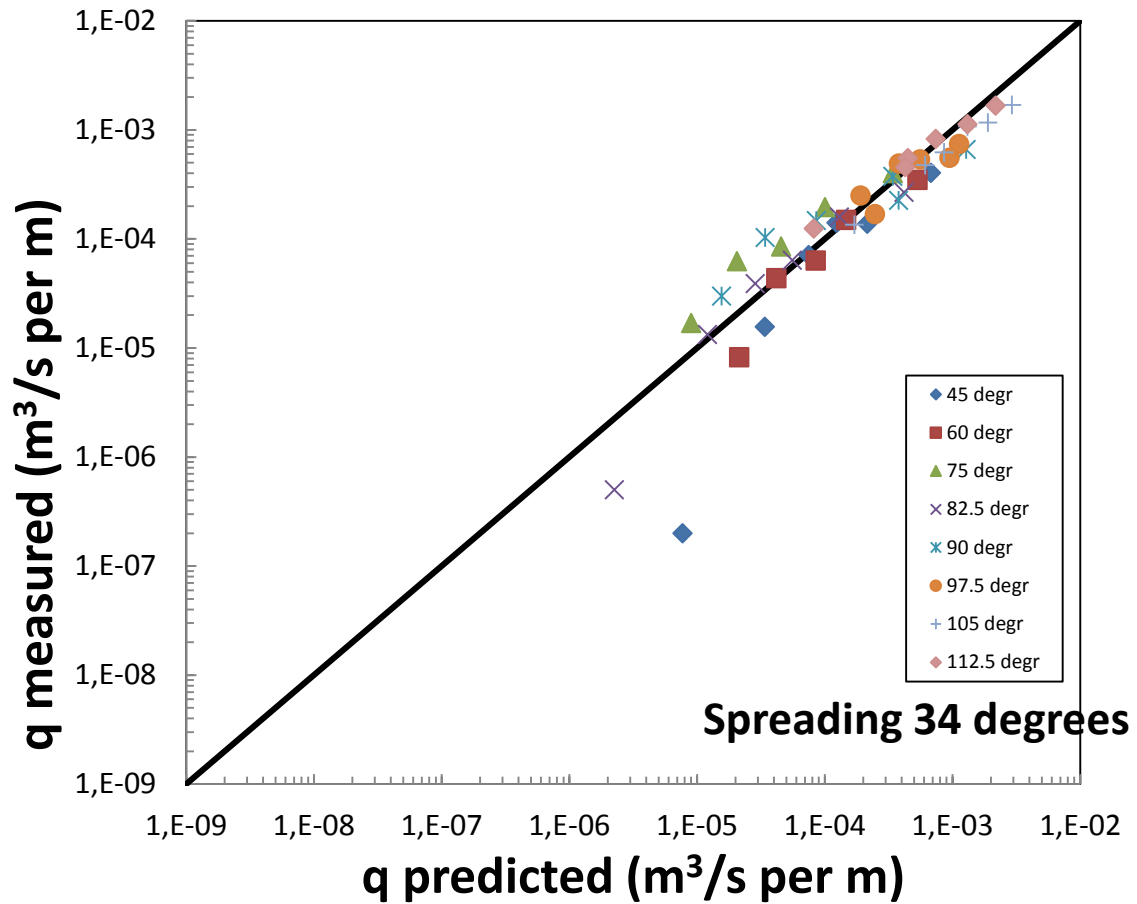
Fig. 6.16.: Graph for predicted vs. measured overtopping, using new adjustment and influence factors, for spreading 34 degrees, for box 4.

Now all values are approximately on the line in the graph. The new design formulae do not let the overtopping for large angles of incidence decrease as fast as the current formulae do, because it has been shown that the overtopping does not decrease so fast and does not become zero at 110°. The wave height and wave period do in fact decrease for large angles of incidence when approaching the dike, but do not become zero.

7. Conclusions and further work

In this chapter the conclusions are given and pointers for further research are described.

7.1. Conclusions

As was mentioned in section 1.2., the goal of this report is: determining the relation between very oblique wave attack and overtopping, and to accordingly adjust the formulae for the oblique wave attack influence and adjustment factors for the wave height and wave period that account for the effect of diffraction.

From the previous chapters a number of conclusions can be derived:

1. Wave overtopping does not decrease as fast as current theory predicts, and also does not become zero for angles of wave attack around 110° and larger. Thus, the theory is on the unsafe side in this area;

2. For overtopping box 5 for known situations (angles of wave attack smaller than 80°) there is a significant difference between measurements and predictions, around a factor 10. This should be analyzed in more depth before further analysis is done;

3. Dimensionless overtopping discharges for a spreading of 34°, for angles of incidence of 45° and 60° were smaller than the values for a spreading of 0° and 12°, which is not according to the theory. Why this difference is present has to be analyzed in more detail;

4. The dimensionless overtopping values for large angles of incidence are of approximately the same magnitude for all three spreading widths, which means that for very large angles of incidence, the influence of the spreading decreases again;

5. There are large differences between the measured values of overtopping boxes 4 and 5, the values of box 5 are much lower. It looks like the distance from the corner of the dike has influence on the overtopping. The influence of diffraction at the corner and the resulting influence on the overtopping have to be studied in more detail;

6. The new design formulae do not let the overtopping for large angles of incidence decrease as fast as the current formulae do. The new empirical design formulae for short-crested waves that were found by iteration, are:
   For oblique wave attack:

$$\gamma_\beta = 1 - 0.0060|\beta| \; ; \; \left(\gamma_\beta \geq 0.60\right) \quad (6.3.)$$

For wave directions $80° < |\beta| \leq 110°$:

$$H_{m0} \text{ is multiplied by } \frac{180-|\beta|}{100} \quad (6.4.)$$

$$T_{m-1,0} \text{ is multiplied by } \sqrt{\frac{180-|\beta|}{100}} \quad (6.5.)$$

A remark to these formulae has to be made. The newly found formulae are empirical and based on the data of one overtopping box. The data has to be studied in more detail to be able to make further adjustments to the theory.

As one can see in section 6.2., overtopping did certainly not become zero at 110° (as the current design formulae predict) and the values for 112.5° were in the same order of magnitude as values for 90° - 105°, which is in accordance with the hypothesis (see section 1.2.). New empirical design formulae were determined in section 6.4. An observation that is not in accordance with the hypothesis is the fact that the overtopping for box 5 for the smaller angles of incidence is significantly lower than theory predicts. This should be studied in more detail, see section 7.2.

7.2. Further work

Some pointers for further work are:

1. The significant difference between measurements and predictions for box 5 for known situations (angles of wave attack smaller than 80°) should be analyzed in more depth before further analysis is to be done;

2. Why the dimensionless overtopping discharges for a spreading of 34°, for angles of incidence of 45° and 60° are smaller than the values for a spreading of 0° and 12 has to be analyzed in more detail;

3. The influence of diffraction at the corner and the resulting influence on the overtopping have to be studied in more detail;

4. The influence of the spreading on overtopping during very large angles of incidence has to be studied in more detail.

Notation

$A(f)$	= function dependent of s, leads to a constant for a certain chosen spreading	[-]
d	= water depth	[m]
$D(f,\theta)$	= the distribution function of directional spreading	[-]
g	= acceleration due to gravity (=9.81)	[m/s^2]
H_{m0}	= estimate of the significant wave height from spectral analysis ($=4\sqrt{m_0}$)	[m]
$L_{m,-1,0}$	= mean wave length in deep water	[m]
q	= average overtopping discharge per meter structure width	[m^3/s/m]
$q_{measured}$	= calculated average overtopping discharge per meter structure width	[m^3/s/m]
$q_{predicted}$	= predicted average overtopping discharge per meter structure width	[m^3/s/m]
R	= wave run-up level	[m]
R_c	= crest freeboard of structure	[m]
$R_{u2\%}$	= run-up level exceeded by 2% of incident waves	[m]
s	= spreading factor (larger than 1)	[-]
s_{0p}	= wave steepness	[-]
$T_{m-1,0}$	= average wave period calculated from spectral moments	[s]
w_x	= wave type indicator	[-]
z	= crest height of structure	[m]
α	= the angle of the structure slope with the horizontal	[°]
β	= angle of wave attack relative to normal on structure	[°]
β_{dike}	= angle of wave attack relative to normal on dike	[°]
$\beta_{wavemaker}$	= angle of wave attack relative to normal on wave maker	[°]
γ_b	= correction factor concerning a berm with width B	[-]
γ_f	= correction factor concerning the roughness and permeability	[-]
γ_v	= correction factor for a vertical wall on top of the crest	[-]
γ_β	= correction factor concerning oblique wave attack	[-]
$\xi_{m-1,0}$	= breaker parameter / surf similarity / Iribarren number	[-]
σ	= spreading width / standard deviation parameter x of normal distribution	[-]
θ	= direction of wave propagation	[°]
θ_m	= main direction of wave propagation	[°]

References

De Waal, J. P., & Van der Meer, J. W. (1990). Invloed van scheve inval en richtingspreiding op golfoploop en overslag (R. T. p. A. Belastingen, Trans.). Delft: Waterloopkundig Laboratorium.

De Waal, J. P., & Van der Meer, J. W. (1992). Wave run-up and overtopping on coastal structures (pp. 1758-1771). Delft: Delft Hydraulics.

Lorke, S., Brüning, A., Bornschein, A., Gilli, S., Krüger, N., Schüttrumpf, H., . . . Werk, S. (2010). Hydralab - FlowDike; Influence of wind and current on wave run-up and wave overtopping (pp. 100). Aachen, Dresden, Brno, Braunschweig.

Pohl, R. (2011). Effect of very oblique Waves on Wave Run-up and Wave Overtopping (CornerDike); Research Proposal for HYDRALAB IV; Shallow Water Basin; Danish Hydraulics Institute (pp. 1). Dresden: Technische Universität Dresden.

Pohl, R., & Krüger, N. (2012a, 06-09-2012). [Data Storage Plan; Effect of very oblique waves on wave run-up and wave overtopping (CornerDike)].

Pohl, R., & Krüger, N. (2012b). [Data Storage Report; Effect of very oblique waves on wave run-up and wave overtopping (CornerDike)].

Pullen, T., Allsop, N. W. H., Bruce, T., Kortenhaus, A., Schüttrumpf, H., & Van der Meer, J. W. (2007). *EurOtop; Wave Overtopping of Sea Defences and Related Structures: Assessment Manual* (Vol. 73): Kuratorium für Forschung im Küstingenieurwesen.

Sand, S. E., & Mynett, A. E. (1987). Directional wave generation and analysis. Lausanne: IAHR seminar.

Van der Meer, J. W. (1998). Wave run-up and overtopping (pp. 15). Enschede: Infram.

Van der Meer, J. W. (2002). Technisch Rapport Golfoploop en Golfoverslag bij Dijken (pp. 53). Delft: Technische Adviescommissie voor de Waterkeringen (TAW).

Van der Meer, J. W. (2012a, 26 September 2012). [Observations tests and first analysis].

Van der Meer, J. W. (2012b, 13 September 2012). [Short crested wave generation].

Van der Meer, J. W. (2012c, June 6, 2012). [Voorstel om Nederland BV te betrekken bij Cornerdike].

Van der Meer, J. W., & Janssen, J. P. F. M. (1994). Wave run-up and wave overtopping at dikes and revetments (pp. 22). Delft: Delft Hydraulics.

Appendix A: Overview of set-up and instruments

CORNERDIKE PLAN
M 1:100
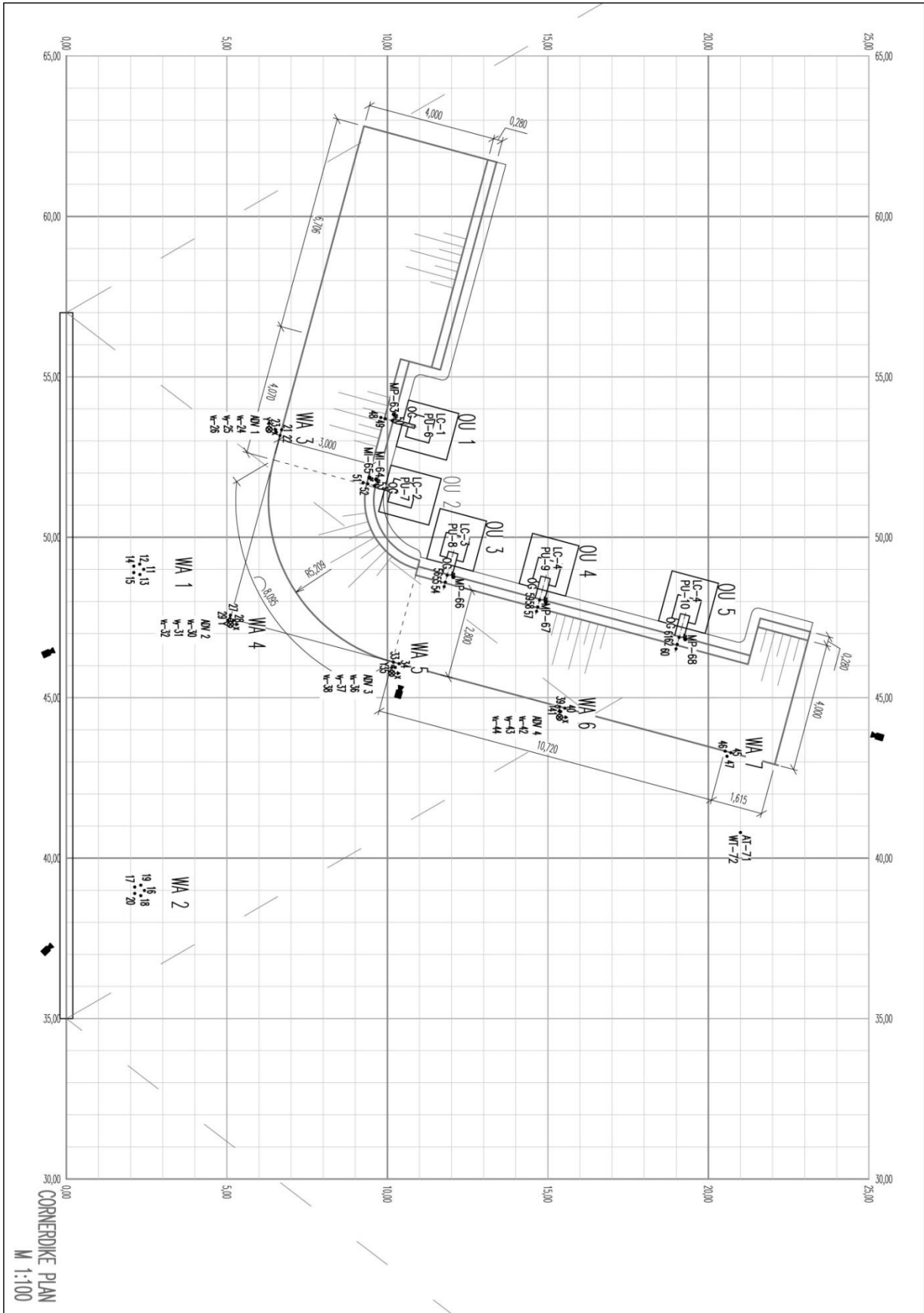
Channel number	Row in *dfs0.file	Description	Position	x-pos. [m]	y-pos. [m]
1	2	Load Cell 1	P-dike, Overtopping-Unit 1	11,5	10
2	3	Load Cell 2	P-dike, Overtopping-Unit 2	14	9,5
3	4	Load Cell 3	Corner, Overtopping-Unit 3	16	11,25
4	5	Load Cell 4	N-dike, Overtopping-Unit 4	17	14,5
5	6	Load Cell 5	N-dike, Overtopping-Unit 5	18	19
6	7	Pump 1	Overtopping-Unit 1	11,5	10
7	8	Pump 2	Overtopping-Unit 2	14	9,5
8	9	Pump 3	Overtopping-Unit 3	16	11,25
9	10	Pump 4	Overtopping-Unit 4	17	14,5
10	11	Pump 5	Overtopping-Unit 5	18	19
11	12	Wave Gauge	Wave Array 1	16	0,5
12	13	Wave Gauge	Wave Array 1	16	0,5
13	14	Wave Gauge	Wave Array 1	16	0,5
14	15	Wave Gauge	Wave Array 1	16	0,5
15	16	Wave Gauge	Wave Array 1	16	0,5
16	17	Wave Gauge	Wave Array 2	25	0,5
17	18	Wave Gauge	Wave Array 2	25	0,5
18	19	Wave Gauge	Wave Array 2	25	0,5
19	20	Wave Gauge	Wave Array 2	25	0,5
20	21	Wave Gauge	Wave Array 2	25	0,5
21	22	Wave Gauge	Wave Array 3	11,75	6,69
22	23	Wave Gauge	Wave Array 3	11,75	6,69
23	24	Wave Gauge	Wave Array 3	11,75	6,69
24	25	ADV v_x	Wave Array 3	11,75	6,69
25	26	ADV v_y	Wave Array 3	11,75	6,69
26	27	ADV v_z	Wave Array 3	11,75	6,69
27	28	Wave Gauge	Wave Array 4	17,54	5,14
28	29	Wave Gauge	Wave Array 4	17,54	5,14
29	30	Wave Gauge	Wave Array 4	17,54	5,14
30	31	ADV v_x	Wave Array 4	17,54	5,14
31	32	ADV v_y	Wave Array 4	17,54	5,14
32	33	ADV v_z	Wave Array 4	17,54	5,14
33	34	Wave Gauge	Wave Array 5	19,1	10,93
34	35	Wave Gauge	Wave Array 5	19,1	10,93
35	36	Wave Gauge	Wave Array 5	19,1	10,93
36	37	ADV v_x	Wave Array 5	19,1	10,93
37	38	ADV v_y	Wave Array 5	19,1	10,93
38	39	ADV v_z	Wave Array 5	19,1	10,93
39	40	Wave Gauge	Wave Array 6	20,65	16,73
40	41	Wave Gauge	Wave Array 6	20,65	16,73
41	42	Wave Gauge	Wave Array 6	20,65	16,73

42	43	ADV v_x	Wave Array 6	20,65	16,73
43	44	ADV v_y	Wave Array 6	20,65	16,73
44	45	ADV v_z	Wave Array 6	20,65	16,73
45	46	Wave Gauge	Wave Array 7	21,69	20,59
46	47	Wave Gauge	Wave Array 7	21,69	20,59
47	48	Wave Gauge	Wave Array 7	21,69	20,59
48	49	Wave Gauge Small	Overtopping-Unit 1	11,5	10
49	50	Wave Gauge Small	Overtopping-Unit 1	11,5	10
50	51	Wave Gauge Small	Overtopping-Unit 1	11,5	10
51	52	Wave Gauge Small	Overtopping-Unit 2	14	9,5
52	53	Wave Gauge Small	Overtopping-Unit 2	14	9,5
53	54	Wave Gauge Small	Overtopping-Unit 2	14	9,5
54	55	Wave Gauge Small	Overtopping-Unit 3	16	11,25
55	56	Wave Gauge Small	Overtopping-Unit 3	16	11,25
56	57	Wave Gauge Small	Overtopping-Unit 3	16	11,25
57	58	Wave Gauge Small	Overtopping-Unit 4	17	14,5
58	59	Wave Gauge Small	Overtopping-Unit 4	17	14,5
59	60	Wave Gauge Small	Overtopping-Unit 4	17	14,5
60	61	Wave Gauge Small	Overtopping-Unit 5	18	19
61	62	Wave Gauge Small	Overtopping-Unit 5	18	19
62	63	Wave Gauge Small	Overtopping-Unit 5	18	19
63	64	Micro-Propeller	Overtopping-Unit 1	11,5	10
64	65	Mini-Propeller	Overtopping-Unit 2	14	9,5
65	66	Mini-Propeller	Overtopping-Unit 2	14	9,5
66	67	Micro-Propeller	Overtopping-Unit 3	16	11,25
67	68	Micro-Propeller	Overtopping-Unit 4	17	14,5
68	69	Micro-Propeller	Overtopping-Unit 5	18	19
69	70	Capacitive Gauge	Cone	11,91	9,59
70	71	Capacitive Gauge	Cone	16,81	12,06
71	72	Air Temperature			
72	73	Water Temperature			

Appendix B: Overview of all the tests and results

	Nominal conditions					Overtopping measured					Gauges 16-20					Calculations						
Test	File-name	Wave no.	wave direction	Water depth	Sop	Load cell 1 (P-Dike)	Load cell 2 (P-Dike)	Load cell 3 (Corner)	Load cell 4 (N-Dike)	Load cell 5 (N-Dike)	Hm0	Tm-1,0	Tp	MWD	DSD	Beta	Rc	Ksim-1,0	gamma B	Hs calc	Tm-1,0 calc	q calc
[-]	[-]	[-]	[°]	[m]	[-]	[l/s/m]	[l/s/m]	[l/s/m]	[l/s/m]	[l/s/m]	[m]	[s]	[s]	[°]	[°]	[°]	[m]	[-]	[-]	[m]	[s]	[l/s/m]
114	ts01_w1_m300_010_60	w1	m300	0,6	0,025	0,029	0,061	0,135	0,071	0,007	0,082	1,379	1,600	17,852	36,713	45	0,10	1,508	0,852	0,082	1,38	0,158
115	ts01_w2_m300_010_60	w2	m300	0,6	0,05	0,002	0,000	0,004	0,000	0,001	0,077	1,040	1,164	15,131	31,836	45	0,10	1,171	0,852	0,077	1,04	0,0216
116	ts01_w3_m300_010_60	w3	m300	0,6	0,025	0,078	0,076	0,370	0,207	0,023	0,094	1,394	1,600	31,022	30,913	45	0,10	1,424	0,852	0,094	1,39	0,259
117	ts01_w4_m300_010_60	w4	m300	0,6	0,05	0,000	0,001	0,024	0,008	0,000	0,083	1,035	1,067	28,857	25,776	45	0,10	1,124	0,852	0,083	1,04	0,0279
136	ts01_w5_m300_010_60	w5	m300	0,6	0,025	0,109	0,067	0,821	0,383	0,022	0,141	1,540	1,829	-4,391	40,088	45	0,10	1,279	0,852	0,141	1,54	1,3
119	ts02_w1_m300_015_60	w1	m300	0,6	0,025	0,434	0,751	0,883	0,404	0,156	0,125	1,611	1,829	19,509	39,355	45	0,10	1,424	0,852	0,125	1,61	1,14
120	ts02_w2_m300_015_60	w2	m300	0,6	0,05	0,119	0,155	0,214	0,141	0,019	0,117	1,215	1,422	15,752	34,544	45	0,10	1,110	0,852	0,117	1,21	0,252
122	ts02_w3_m300_015_60	w3	m300	0,6	0,025	0,783	0,939	1,946	0,966	0,307	0,146	1,627	1,829	30,499	35,330	45	0,10	1,328	0,852	0,146	1,63	1,77
123	ts02_w4_m300_015_60	w4	m300	0,6	0,05	0,164	0,186	0,488	0,327	0,044	0,137	1,228	1,422	29,890	28,483	45	0,10	1,035	0,852	0,137	1,23	0,439
148	ts02_w5_m300_015_60	w5	m300	0,6	0,025	0,497	1,010	2,810	1,181	0,208	0,155	1,615	1,829	33,078	32,699	45	0,10	1,282	0,852	0,155	1,61	1,97
164	ts03_w1_m300_007_65	w1	m300	0,65	0,025	0,030	0,031	0,297	0,138	0,057	0,055	1,204	1,280	12,281	38,475	45	0,05	1,607	0,852	0,055	1,20	0,365
165	ts03_w2_m300_007_65	w2	m300	0,65	0,05	0,001	0,002	0,037	0,016	0,001	0,050	0,904	0,914	12,916	29,977	45	0,05	1,264	0,852	0,050	0,90	0,0708
166	ts03_w3_m300_007_65	w3	m300	0,65	0,025	0,063	0,053	0,536	0,291	0,112	0,062	1,208	1,280	29,465	32,959	45	0,05	1,518	0,852	0,062	1,21	0,499
167	ts03_w4_m300_007_65	w4	m300	0,65	0,05	0,001	0,004	0,093	0,055	0,007	0,055	0,909	0,985	26,431	24,253	45	0,05	1,211	0,852	0,055	0,91	0,0995
101	ts04_w1_m150_010_60	w1	m150	0,6	0,025	0,027	0,075	0,105	0,044	0,009	0,086	1,373	1,600	44,267	44,267	60	0,10	1,467	0,802	0,086	1,37	0,137
102	ts04_w2_m150_010_60	w2	m150	0,6	0,05	0,000	0,001	0,000	0,000	0,000	0,084	1,029	1,164	7,274	37,265	60	0,10	1,108	0,802	0,084	1,03	0,0198
132	ts04_w5_m150_010_60	w5	m150	0,6	0,025	0,222	0,191	0,127	0,220	0,173	0,093	1,343	1,600	14,259	33,579	60	0,10	1,377	0,802	0,093	1,34	0,159
104	ts05_w1_m150_015_60	w1	m150	0,6	0,025	0,474	0,874	0,711	0,347	0,206	0,133	1,632	1,829	10,403	47,105	60	0,10	1,396	0,802	0,133	1,63	1,19
105	ts05_w2_m150_015_60	w2	m150	0,6	0,05	0,085	0,190	0,121	0,063	0,007	0,129	1,207	1,422	7,643	40,844	60	0,10	1,051	0,802	0,129	1,21	0,257
161	ts05_w3_m150_015_60	w3	m150	0,6	0,025	1,106	1,765	1,578	0,926	0,746	0,149	1,610	2,133	19,861	38,414	60	0,10	1,303	0,802	0,149	1,61	1,49
133	ts05_w5_m150_015_60	w5	m150	0,6	0,025	1,388	1,553	0,787	0,888	1,095	0,154	1,638	1,829	16,554	32,574	60	0,10	1,303	0,802	0,154	1,64	1,73
168	ts06_w1_m150_007_65	w1	m150	0,65	0,025	0,033	0,039	0,261	0,150	0,060	0,059	1,183	1,280	8,618	36,701	60	0,05	1,521	0,802	0,059	1,18	0,337
169	ts06_w2_m150_007_65	w2	m150	0,65	0,05	0,001	0,001	0,030	0,008	0,002	0,054	0,895	0,914	6,999	31,114	60	0,05	1,201	0,802	0,054	0,90	0,0675
192	ts06_w4_m150_007_65	w4	m150	0,65	0,05	0,001	0,001	0,069	0,061	0,026	0,062	0,877	0,914	11,659	24,255	60	0,05	1,097	0,802	0,062	0,88	0,0954
107	ts07_w1_p000_010_60	w1	p000	0,6	0,025	0,026	0,099	0,103	0,063	0,016	0,090	1,380	1,600	-1,514	46,108	75	0,10	1,437	0,753	0,090	1,38	0,124
108	ts07_w2_p000_010_60	w2	p000	0,6	0,05	0,001	0,002	0,002	0,000	0,000	0,085	1,037	1,164	0,331	37,926	75	0,10	1,107	0,753	0,085	1,04	0,0148
134	ts07_w5_p000_010_60	w5	p000	0,6	0,025	0,069	0,299	0,010	0,008	0,004	0,097	1,323	1,600	-2,369	33,344	75	0,10	1,329	0,753	0,097	1,32	0,124
111	ts08_w1_p000_015_60	w1	p000	0,6	0,025	0,409	0,933	0,740	0,400	0,240	0,142	1,632	1,829	3,834	48,842	75	0,10	1,351	0,753	0,142	1,63	1,14
112	ts08_w2_p000_015_60	w2	p000	0,6	0,05	0,100	0,199	0,134	0,085	0,020	0,137	1,211	1,422	0,622	42,726	75	0,10	1,022	0,753	0,137	1,21	0,239
162	ts08_w3_p000_015_60	w3	p000	0,6	0,025	0,678	1,642	0,403	0,231	0,348	0,149	1,575	1,829	0,330	41,550	75	0,10	1,274	0,753	0,149	1,58	1,11
135	ts08_w5_p000_015_60	w5	p000	0,6	0,025	0,584	1,780	0,206	0,073	0,073	0,141	1,540	1,829	-4,391	40,088	75	0,10	1,279	0,753	0,141	1,54	0,869
170	ts09_w1_p000_007_65	w1	p000	0,65	0,025	0,030	0,049	0,290	0,196	0,062	0,063	1,194	1,280	0,036	37,961	75	0,05	1,482	0,753	0,063	1,19	0,344
171	ts09_w2_p000_007_65	w2	p000	0,65	0,05	0,001	0,001	0,038	0,017	0,006	0,056	0,891	0,914	0,450	32,832	75	0,05	1,181	0,753	0,056	0,89	0,0527
191	ts09_w4_p000_007_65	w4	p000	0,65	0,05	0,001	0,000	0,014	0,012	0,004	0,066	0,862	0,985	-1,107	27,545	75	0,05	1,045	0,753	0,066	0,86	0,0794
126	ts10_w1_p075_010_60	w1	p075	0,6	0,025	0,018	0,060	0,075	0,039	0,018	0,090	1,375	1,600	-0,250	41,095	82,5	0,10	1,432	0,736	0,082	1,32	0,0601
127	ts10_w2_p075_010_60	w2	p075	0,6	0,05	0,001	0,001	0,001	0,001	0,000	0,087	1,033	1,164	-2,748	34,677	82,5	0,10	1,094	0,736	0,080	0,99	0,00637
131	ts10_w5_p075_010_60	w5	p075	0,6	0,025	0,013	0,151	0,001	0,000	0,004	0,100	1,382	1,600	-6,474	37,143	82,5	0,10	1,366	0,736	0,092	1,32	0,0916
139	ts11_w1_p075_015_60	w1	p075	0,6	0,025	0,322	0,719	0,520	0,268	0,187	0,143	1,618	1,829	-2,306	43,950	82,5	0,10	1,337	0,736	0,131	1,55	0,668
140	ts11_w2_p075_015_60	w2	p075	0,6	0,05	0,080	0,165	0,111	0,064	0,013	0,135	1,198	1,422	-0,664	38,580	82,5	0,10	1,019	0,736	0,124	1,15	0,111
141	ts11_w5_p075_015_60	w5	p075	0,6	0,025	0,156	0,945	0,039	0,015	0,008	0,143	1,528	1,829	-12,258	40,675	82,5	0,10	1,262	0,736	0,131	1,46	0,509
143	ts11_w6_p075_015_60	w6	p075	0,6	0,05	0,097	0,405	0,000	0,000	0,000	0,144	1,198	1,422	-5,684	29,355	82,5	0,10	0,987	0,736	0,132	1,15	0,139
172	ts12_w1_p075_007_65	w1	p075	0,65	0,025	0,020	0,035	0,235	0,159	0,059	0,064	1,194	1,280	-4,718	39,016	82,5	0,05	1,475	0,736	0,059	1,14	0,209
173	ts12_w2_p075_007_65	w2	p075	0,65	0,05	0,000	0,001	0,027	0,013	0,003	0,054	0,896	0,914	-3,246	34,436	82,5	0,05	1,202	0,736	0,050	0,86	0,0252
149	ts13_w1_p150_010_60	w1	p150	0,6	0,025	0,010	0,037	0,040	0,030	0,008	0,090	1,380	1,600	-6,423	41,655	90	0,10	1,437	0,736	0,060	1,13	0,005
150	ts13_w3_p150_010_60	w3	p150	0,6	0,025	0,008	0,057	0,003	0,005	0,015	0,094	1,357	1,600	-13,618	39,350	90	0,10	1,379	0,736	0,063	1,11	0,00543

151	ts13_w5_p150_010_60	w5	p150	0,6	0,025	0,002	0,022	0,000	0,000	0,001	0,098	1,370	1,600	-14,205	42,349	90	0,10	1,370	0,736	0,065	1,12	0,00681
175	ts14_w2_p150_010_65	w2	p150	0,65	0,05	0,026	0,041	0,173	0,147	0,068	0,084	1,031	1,164	-6,616	36,027	90	0,05	1,114	0,736	0,056	0,84	0,0339
176	ts14_w4_p150_010_65	w4	p150	0,65	0,05	0,035	0,079	0,035	0,054	0,023	0,088	1,016	1,164	-12,964	29,043	90	0,05	1,067	0,736	0,059	0,83	0,0382
177	ts14_w6_p150_010_65	w6	p150	0,65	0,05	0,018	0,071	0,009	0,011	0,004	0,087	1,027	1,164	-14,750	18,285	90	0,05	1,090	0,736	0,058	0,84	0,0378
152	ts15_w1_p150_015_60	w1	p150	0,6	0,025	0,346	0,782	0,619	0,374	0,324	0,151	1,647	1,829	-6,426	44,116	90	0,10	1,326	0,736	0,100	1,35	0,139
153	ts15_w2_p150_015_60	w2	p150	0,6	0,05	0,102	0,179	0,129	0,103	0,028	0,136	1,212	1,422	-5,679	40,067	90	0,10	1,026	0,736	0,091	0,99	0,0115
154	ts15_w3_p150_015_60	w3	p150	0,6	0,025	0,196	0,700	0,083	0,051	0,093	0,153	1,615	1,829	-15,568	41,420	90	0,10	1,291	0,736	0,102	1,32	0,13
155	ts15_w4_p150_015_60	w4	p150	0,6	0,05	0,088	0,197	0,004	0,006	0,005	0,145	1,198	1,422	-12,386	34,428	90	0,10	0,984	0,736	0,096	0,98	0,0138
156	ts15_w5_p150_015_60	w5	p150	0,6	0,025	0,047	0,339	0,018	0,007	0,007	0,154	1,593	1,829	-20,855	41,782	90	0,10	1,266	0,736	0,103	1,30	0,124
157	ts15_w6_p150_015_60	w6	p150	0,6	0,05	0,044	0,189	0,000	0,000	0,001	0,135	1,203	1,422	-15,744	28,972	90	0,10	1,021	0,736	0,090	0,98	0,0106
193	ts16_w1_p150_007_68	w1	p150	0,68	0,025	0,097	0,174	0,793	0,661	0,370	0,063	1,194	1,280	-9,362	39,238	90	0,02	1,489	0,736	0,042	0,98	0,673
194	ts16_w2_p150_007_68	w2	p150	0,68	0,05	0,002	0,002	0,276	0,226	0,148	0,055	0,898	0,914	-9,677	34,710	90	0,02	1,199	0,736	0,037	0,73	0,184
195	ts16_w3_p150_007_68	w3	p150	0,68	0,025	0,090	0,223	0,643	0,687	0,298	0,066	1,168	1,280	-14,140	34,094	90	0,02	1,417	0,736	0,044	0,95	0,702
196	ts16_w4_p150_007_68	w4	p150	0,68	0,05	0,001	0,014	0,125	0,150	0,119	0,062	0,885	0,985	-14,661	27,085	90	0,02	1,114	0,736	0,041	0,72	0,232
197	ts16_w5_p150_007_68	w5	p150	0,68	0,025	0,033	0,184	0,370	0,557	0,120	0,066	1,155	1,280	-16,263	36,835	90	0,02	1,401	0,736	0,044	0,94	0,681
198	ts16_w6_p150_007_68	w6	p150	0,68	0,05	0,003	0,023	0,096	0,160	0,057	0,057	0,888	0,985	-14,863	17,285	90	0,02	1,163	0,736	0,038	0,72	0,193
158	ts17_w1_p225_015_60	w1	p225	0,6	0,025	0,257	0,522	0,469	0,250	0,238	0,148	1,651	1,829	-11,400	44,949	97,5	0,10	1,341	0,736	0,062	1,07	0,00349
159	ts17_w3_p225_015_60	w3	p225	0,6	0,025	0,050	0,227	0,030	0,025	0,051	0,149	1,600	1,829	-19,611	40,384	97,5	0,10	1,293	0,736	0,062	1,03	0,00276
160	ts17_w5_p225_015_60	w5	p225	0,6	0,025	0,018	0,061	0,006	0,009	0,005	0,153	1,602	1,829	-18,622	41,146	97,5	0,10	1,278	0,736	0,064	1,03	0,00317
185	ts18_w2_p225_015_65	w2	p225	0,65	0,05	0,269	0,542	0,667	0,535	0,436	0,137	1,224	1,422	-13,228	41,397	97,5	0,05	1,032	0,736	0,057	0,79	0,0249
186	ts18_w4_p225_015_65	w4	p225	0,65	0,05	0,201	0,479	0,113	0,156	0,193	0,146	1,206	1,422	-21,169	34,404	97,5	0,05	0,987	0,736	0,061	0,78	0,0282
187	ts18_w6_p225_015_65	w6	p225	0,65	0,05	0,099	0,236	0,038	0,045	0,088	0,145	1,211	1,280	-21,175	33,216	97,5	0,05	0,993	0,736	0,060	0,78	0,0285
182	ts19_w1_p225_010_65	w1	p225	0,65	0,025	0,134	0,280	0,624	0,491	0,289	0,096	1,398	1,600	-14,946	43,446	97,5	0,05	1,410	0,736	0,040	0,90	0,0154
183	ts19_w3_p225_010_65	w3	p225	0,65	0,025	0,035	0,106	0,169	0,196	0,285	0,097	1,370	1,600	-22,207	40,156	97,5	0,05	1,377	0,736	0,040	0,88	0,0138
184	ts19_w5_p225_010_65	w5	p225	0,65	0,025	0,014	0,032	0,058	0,091	0,210	0,095	1,377	1,600	-22,680	45,326	97,5	0,05	1,397	0,736	0,039	0,89	0,0133
204	ts20_w2_p225_010_68	w2	p225	0,68	0,05	0,110	0,178	0,779	0,741	0,522	0,085	1,030	1,164	-13,265	36,980	97,5	0,02	1,101	0,736	0,036	0,67	0,115
205	ts20_w4_p225_010_68	w4	p225	0,68	0,05	0,066	0,182	0,343	0,521	0,258	0,090	1,020	1,067	-21,969	30,352	97,5	0,02	1,061	0,736	0,038	0,66	0,127
199	ts21_w1_p225_007_68	w1	p225	0,68	0,025	0,073	0,118	0,718	0,556	0,332	0,063	1,192	1,280	-13,245	40,769	97,5	0,02	1,484	0,736	0,026	0,77	0,0959
200	ts21_w2_p225_007_68	w2	p225	0,68	0,05	0,002	0,005	0,214	0,168	0,111	0,053	0,900	0,985	-13,191	35,405	97,5	0,02	1,217	0,736	0,022	0,58	0,0145
201	ts21_w3_p225_007_68	w3	p225	0,68	0,025	0,025	0,102	0,431	0,543	0,165	0,066	1,192	1,280	-20,908	36,571	97,5	0,02	1,450	0,736	0,028	0,77	0,109
202	ts21_w4_p225_007_68	w4	p225	0,68	0,05	0,001	0,006	0,132	0,152	0,103	0,058	0,899	0,914	-19,592	28,245	97,5	0,02	1,164	0,736	0,024	0,58	0,019
188	ts22_w1_p300_015_65	w1	p300	0,65	0,025	0,455	1,051	1,511	1,079	1,051	0,143	1,639	1,829	-15,521	45,826	105	0,05	1,354	0,736	0,024	0,67	0,0000948
189	ts22_w3_p300_015_65	w3	p300	0,65	0,025	0,088	0,245	0,375	0,298	0,477	0,149	1,634	1,829	-29,704	44,443	105	0,05	1,322	0,736	0,025	0,67	0,000117
214	ts23_w2_p300_015_68	w2	p300	0,68	0,05	0,689	1,166	1,775	1,688	1,308	0,129	1,229	1,422	-18,194	41,214	105	0,02	1,069	0,736	0,021	0,50	0,00512
215	ts23_w4_p300_015_68	w4	p300	0,68	0,05	0,369	0,768	0,885	1,186	0,980	0,139	1,220	1,422	-31,362	34,806	105	0,02	1,022	0,736	0,023	0,50	0,00646
210	ts24_w1_p300_010_68	w1	p300	0,68	0,025	0,236	0,444	1,229	1,167	0,600	0,087	1,367	1,600	-19,862	43,379	105	0,02	1,448	0,736	0,014	0,56	0,00226
211	ts24_w2_p300_010_68	w2	p300	0,68	0,05	0,090	0,135	0,674	0,621	0,451	0,086	1,050	1,164	-17,082	38,590	105	0,02	1,118	0,736	0,014	0,43	0,000256
212	ts24_w3_p300_010_68	w3	p300	0,68	0,025	0,101	0,154	0,954	1,122	0,724	0,089	1,387	1,600	-31,194	37,248	105	0,02	1,451	0,736	0,015	0,57	0,00278
213	ts24_w4_p300_010_68	w4	p300	0,68	0,05	0,011	0,047	0,249	0,405	0,141	0,084	1,048	1,164	-31,331	31,063	105	0,02	1,131	0,736	0,014	0,43	0,00022
206	ts25_w1_p300_007_68	w1	p300	0,68	0,025	0,044	0,089	0,599	0,476	0,271	0,060	1,194	1,280	-19,452	41,478	105	0,02	1,521	0,736	0,010	0,49	0,000136
207	ts25_w2_p300_007_68	w2	p300	0,68	0,05	0,000	0,001	0,181	0,135	0,078	0,054	0,911	0,985	-17,289	35,197	105	0,02	1,228	0,736	0,009	0,37	0,00000351
208	ts25_w3_p300_007_68	w3	p300	0,68	0,025	0,003	0,032	0,304	0,434	0,093	0,064	1,188	1,280	-28,831	34,064	105	0,02	1,466	0,736	0,011	0,48	0,000178
209	ts25_w4_p300_007_68	w4	p300	0,68	0,05	0,000	0,004	0,057	0,066	0,040	0,055	0,919	0,985	-26,961	28,733	105	0,02	1,222	0,736	0,009	0,38	0,00000469
222	ts25_w5_p300_007_68	w5	p300	0,68	0,025	0,001	0,006	0,250	0,493	0,102	0,063	1,198	1,280	-27,781	41,402	105	0,02	1,489	0,736	0,011	0,49	0,000181
223	ts25_w6_p300_007_68	w6	p300	0,68	0,05	0,000	0,000	0,047	0,076	0,013	0,053	0,916	0,914	-29,270	17,992	105	0,02	1,249	0,736	0,009	0,37	0,00
190	ts26_w1_p375_015_65	w1	p375	0,65	0,025	0,298	0,682	1,128	0,827	0,853	0,137	1,638	1,829	-22,818	47,169	112,5	0,05	1,383	0,736	0,000	0,00	0,00
221	ts27_w2_p375_015_68	w2	p375	0,68	0,05	0,575	0,958	1,684	1,666	1,079	0,130	1,237	1,422	-23,753	40,842	112,5	0,02	1,071	0,736	0,000	0,00	0,00
219	ts28_w1_p375_010_68	w1	p375	0,68	0,025	0,212	0,350	1,326	1,128	0,635	0,085	1,376	1,600	-29,803	41,547	112,5	0,02	1,474	0,736	0,000	0,00	0,00
220	ts28_w2_p375_010_68	w2	p375	0,68	0,05	0,052	0,088	0,610	0,552	0,356	0,077	1,047	1,164	-24,375	39,094	112,5	0,02	1,176	0,736	0,000	0,00	0,00
216	ts29_w1_p375_007_68	w1	p375	0,68	0,025	0,028	0,065	0,557	0,455	0,242	0,060	1,217	1,280	-31,620	39,767	112,5	0,02	1,552	0,736	0,000	0,00	0,00
217	ts29_w2_p375_007_68	w2	p375	0,68	0,05	0,001	0,001	0,186	0,125	0,072	0,050	0,908	0,985	-22,042	36,611	112,5	0,02	1,268	0,736	0,000	0,00	0,00
224	ts29_w6_p375_007_68	w6	p375	0,68	0,05	0,000	0,001	0,001	0,000	0,000	0,030	0,942	0,985	-37,162	26,526	112,5	0,02	1,687	0,736	0,000	0,00	0,00